

AD-A220 996

DTIC FILE COPY REPORT DOCUMENTATION PAGE			Form Approved OMB No. 0704-0188	
<small>Public reporting burden for this collection of information is estimated to average 1 hour per response, including the time for reviewing instructions, searching existing data sources, gathering and maintaining the data needed, and completing and reviewing the collection of information. Send comments regarding this burden estimate or any other aspect of this collection of information, including suggestions for reducing the burden, to Washington Headquarters Services, Directorate for Information Operations and Reports, 1215 Jefferson Davis Highway, Suite 1204, Arlington, VA 22202-4302, and to the Office of Management and Budget, Paperwork Reduction Project (0704-0188), Washington, DC 20503.</small>				
1. AGENCY USE ONLY (Leave blank)		2. REPORT DATE March 1990	3. REPORT TYPE AND DATES COVERED Final Report 6/15/86 - 6/14/89	
4. TITLE AND SUBTITLE Direct Writing of Microstructures for Solid-State Electronics			5. FUNDING NUMBERS (2) 61102F/2301/A1	
6. AUTHOR(S) Richard M. Osgood, Dragan Podlesnik, Rob Scarmozzino			7. PERFORMING ORGANIZATION NAME(S) AND ADDRESS(ES) Columbia University Microelectronics Sciences Laboratories 500 West 120th St. 253 Engineering Terrace New York, NY 10027 AFOSR-TR-90-0512	
8. SPONSORING/MONITORING AGENCY NAME(S) AND ADDRESS(ES) Airforce Office of Scientific Research/NP Building 410 Bolling AFB, DC 20332-6448			9. SPONSORING/MONITORING AGENCY REPORT NUMBER F49620-86-C-0067	
10. SUPPLEMENTARY NOTES				
11. DISTRIBUTION/AVAILABILITY STATEMENT <i>Approved for public release</i> Distribution Unlimited			12. DISTRIBUTION CODE	
13. ABSTRACT (Maximum 200 words) Progress in using laser chemical processing for several applications in microelectronics and integrated optics is described. These applications are direct writing of metal interconnects on silicon integrated circuits; laser doping, etching and surface modification of GaAs, and fabrication of light guiding components for integrated optics.				
14. SUBJECT TERMS laser processing, Optical Coupler, diffraction grating, laser, GaAs, Si, Integrated Optics, Integrated Circuits, Aluminum Metallization, Shallow doping, Waveguides,				
15. SECURITY CLASSIFICATION OF REPORT unclassified		16. SECURITY CLASSIFICATION OF THIS PAGE unclassified		17. SECURITY CLASSIFICATION OF ABSTRACT unclassified
18. LIMITATION OF ABSTRACT UL SAR		19. NUMBER OF PAGES 42		
20. PRICE CODE		21. LIMITATION OF ABSTRACT		

[illegible]

Richard M. Osgood  
Columbia University  
Microelectronics Sciences Laboratories  
500 West 120th Street  
253 Engineering Terrace  
New York, NY 10027

Final Technical Report for Period  
06/15/86 - 06/14/89

Prepared For  
USAF, AFSC  
Air Force office of Scientific Research  
Building 410  
Bolling AFB DC 20332-6448

Sponsored by  
Advanced Research Projects Agency (DOD)  
ARPA Order No. 9107  
Monitored by AFOSR Under Contract #F49620-86-C-0067

## Table of Contents

I. Introduction. . . . .	1
II. Laser Direct Writing of Metals. . . . .	2
III. Laser Processing of GaAs . . . . .	6
IV. Laser Writing of Integrated Optical Components . . . . .	15
Publications. . . . .	37

Accession For	
NTIS - CRA&I	<input checked="" type="checkbox"/>
DTIC - TAB	<input type="checkbox"/>
Unannounced	<input type="checkbox"/>
Justification	
By	
Distribution /	
Availability Codes	
Dist	Availability Code Special
A-1	



## 1. Introduction

### A. Objective

This report describes a three-year research effort to extend the techniques and applications of laser direct writing to GaAs devices and circuits, and, in addition, to explore new approaches to using this form of maskless processing for integrated optical devices and structures. Strong emphasis was given to the development of novel processing options. In addition, the increased instrumentation capability in the Columbia Microelectronics Sciences Laboratories also allowed a greater opportunity for the exploration of specific applications.

### B. Background

Since its first discovery, maskless fabrication based on laser processing has become an important potential and actual tool in modern microelectronics fabrication. Laser-deposited metals for photolithographic mask repair have been demonstrated by several semiconductor manufacturers, and the commercial sales of machines based on such technology are beginning. Exploration of laser direct-write metallization for package repair and engineering changes has been pursued at IBM; a program which included a collaborative project with Columbia University. IBM and Toshiba have used excimer laser etching for maskless patterning in package and I.C. manufacture. The latter company, in fact, demonstrated the manufacture of a 64 KBit RAM, using excimer-driven  $\text{Cl}_2$  etching of silicon. Both Lincoln Lab and Lawrence Livermore have demonstrated using laser-direct write etching and metallization for interconnection and alteration of gate arrays and ring oscillators. Recently several companies, e.g. LASA, n-chip, and Laserpath have used laser writing in various forms in commercial instruments for ASIC manufacture.

In general, however, there has been little attempt to apply laser processing technology to GaAs. Part of the difficulty is that most programs have emphasized high-temperature thermal processes. This approach is unsatisfactory on GaAs because of the disproportionation of GaAs into gallium and arsenic at relatively low-temperatures,  $< 400^\circ\text{C}$ . Because of yield problems in GaAs devices and the geometry of gallium arsenide circuits, direct writing can play a major role in yield enhancement and circuit optimization. However, in order to do satisfactory exploration of this area, many basic studies need to be accomplished, including determination of the appropriate technique for etching and deposition of materials.

In addition, laser maskless fabrication can be used extensively to make integrated optical structures. Prior to the work described here, however, the previous research has been more concentrated in the areas of  $\text{LiNbO}_3$  waveguide technology and GaAs planar gratings. There has been little or no effort to apply these new techniques to the development of devices for the more usual integrated optical materials such as InP and its related alloys. In these materials, structures are more complex and the surface reactions considerably different in nature than either GaAs and  $\text{LiNbO}_3$ . As a result, the feasibility and the limits for maskless laser fabrication need to be explored in this area.

## II. Laser Direct Writing of Metals

During our current research, significant progress has been made in advancing the technology and feasibility of direct writing and other forms of laser processing on silicon and GaAs.

### A. Development of High Conductivity, Low-Temperature Metal Interconnects

Modern integrated circuits are fragile composites of thin dielectric layers and narrowly or abruptly doped regions. In attempting to develop microtools for altering or reconfiguring these modern chips, it is essential to have a low-temperature direct writing technique. The most commonly applied, direct writing techniques, at the time of this contract, used microthermal chemistry. Unfortunately, some of the most useful molecular precursors, such as Si, are not compatible with the usual high conductivity metals, chiefly aluminum, for silicon IC's.

In the present contract, we have succeeded in demonstrating that good, conductive interconnects can be written with aluminum on Si,  $\text{SiO}_2$  and GaAs. In addition, we have shown the application of laser writing to repair of packages for electronics.

### B. Laser Direct Writing of Aluminum for Silicon IC's

Although aluminum is by far the most common conductor metal in integrated circuits, it had not previously been possible to direct-write highly conductive aluminum from any known metallorganic source. Intrinsically low deposition rates from compounds such as  $\text{TMAI}$  and  $\text{TIBA1}$  lead to a high degree of oxidation of the deposited film and the dissociation chemistry is such that high carbon incorporation from the organic ligands occurs.

We have demonstrated the first successful direct writing of aluminum lines of high conductivity using dimethylaluminum hydride ( $\text{DMAIH}$ ) as the metallorganic parent gas and a

257-nm focused beam, obtained from a frequency-doubled, argon-ion laser. We attribute the purity of the deposited lines partly to the new metallorganic source, DMAIH, which decomposes without any apparent carbon inclusions, and partly to our relatively high-power UV laser source (which leads to a hybrid photolytic/pyrolytic deposition scheme).

In our experiments, the laser sources were an  $\text{Ar}^+$  laser at 514.5 nm or at 350 nm, or the frequency-doubled  $\text{Ar}^+$  laser. The latter source was obtained by an intracavity frequency doubler at 257nm. With these multiple sources, it was possible to compare the quality of the deposited material using a pyrolytic mechanism to that obtained using a photolytic one. With the relatively high intensity, deep-UV laser, viz powers  $\sim 60$  mW, a hybrid deposition scheme results. In this case, a combination of both photodeposition and pyrolytic growth occurred.

In the experiments, *in situ* resistance measurements of the deposited metal lines were made by prepatterned test structures on the substrates and connecting them to the outside with electrical feedthroughs. With this set up, we have obtained values that are only 2-3 times the resistivity of bulk aluminum. Figure 1 shows the line resistivity with respect to bulk aluminum resistivity (Q) versus incident laser power. Laser intensities of more than  $25 \text{ kW/cm}^2$  were necessary to obtain low-resistance aluminum lines.

In addition, using this technique, it has been possible to obtain low contact resistance between these laser written lines and evaporated aluminum patterns that were previously exposed to air and included a native oxide. Electrical contact through this native oxide has been a drawback of low-temperature laser direct writing, since one could not make good connections with the pre-existing aluminum patterns that are found on a conventionally processed IC. Experiments on actual IC structures were demonstrated for this purpose.

### C. Discretionary Writing of Interconnects for Repair of Polyimide Advanced Electronic

#### Packaging

The goal of this project was to develop a low-temperature, direct-writing technique suited to repairing a small number of defects in the packaging circuitry commonly used on wafer-based packaging at Bell Labs in Murray Hill, NJ. These defects are typically breaks in Cu-based lines on a polyimide/semiconductor base, which occur after thermal cycling of the wafer due to the difference between the metal's and semiconductor's thermal expansion coefficients. While these breaks can occur anywhere, they are typically found towards the edges of a wafer where the accumulated stresses are the greatest. Repair of these defects consists of reconnecting the Cu

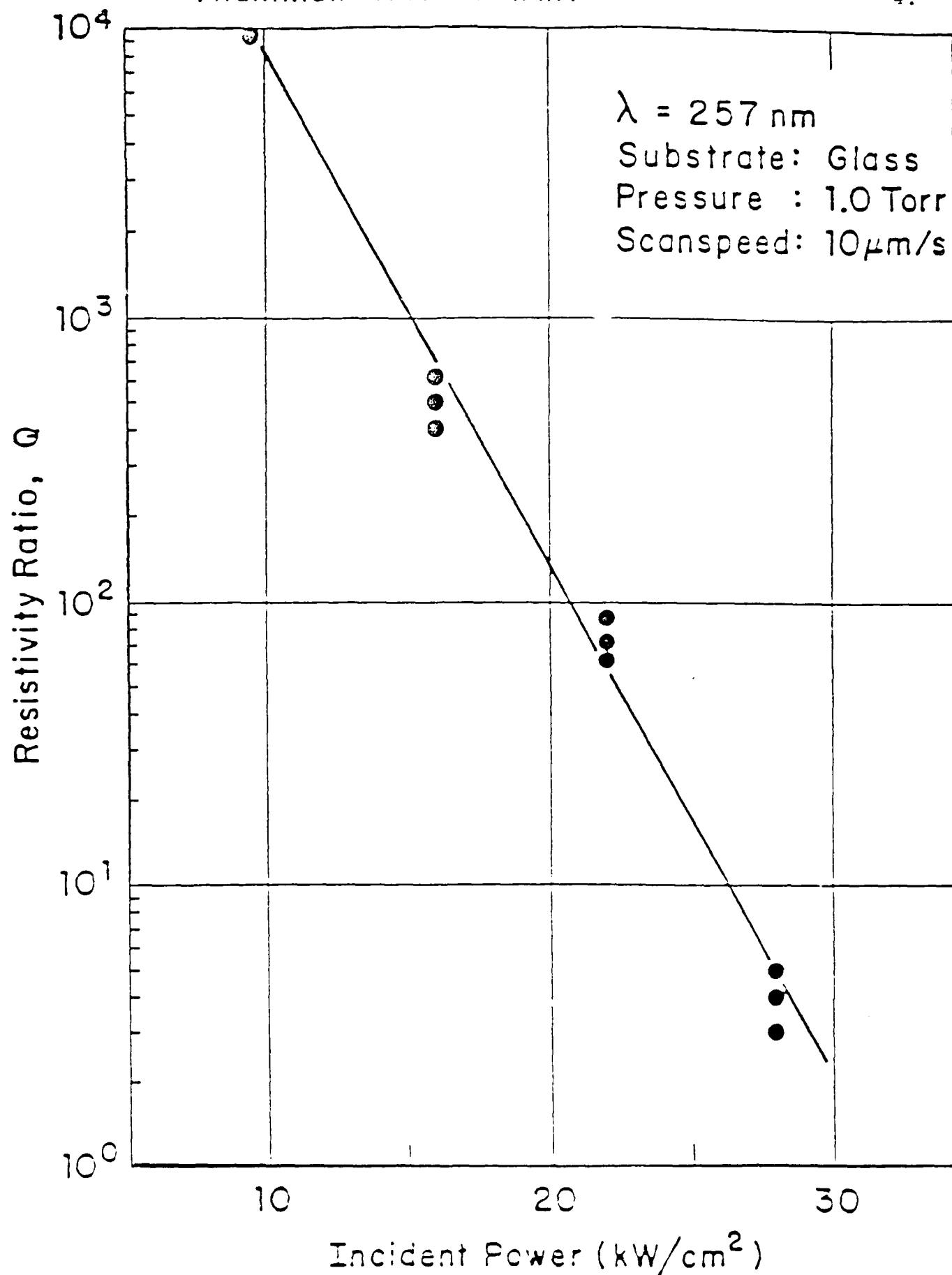


Fig. 1 Line resistivity with respect to bulk aluminum resistivity ( $Q$ ) versus incident laser power.

lines. Note that a successful repair technology can also be used to accomplish design changes on the package during the design phase, as circuits can be shorted or redrawn at will.

Previous attempts in this area have been made by workers at Bell Labs, who investigated using a thermally activated laser-deposition process to write the connecting metal. In this approach, a spin-on coating of a metal-containing gas source is applied to the wafer. Then, a high power, visible, focussed laser beam is used to heat the coated surface to some critical temperature, thereby curing the metal. For this particular defect, this approach was unsuccessful. It was found that sufficient deposition to ensure coverage of the 2.5-25  $\mu\text{m}$  high steps between the broken lines and the polyimide/Si base could not be attained for several reasons. First, heat sinking by the preexisting Cu lines inhibited curing of the film in the vicinity of these lines. Similarly, the amount of metal that could be deposited in any area was limited to 1000 Å. Finally, the thickness of the spin-on film was even less in the most critical areas, the steps themselves, a problem similar to that encountered by those who employ conventional photolithographic processing involving spin-on resists.

For these reasons, we decided to apply a photolytic deposition process to the problem. In this case, the organometallic gas is dissociated non-thermally using a very low power, ultraviolet laser. As the source is continually replenished, the metal can be written in any pattern or thickness, independent of substrate heat sinking effects. The organometallic gases dimethylzinc (DMZn) and diethylzinc (DEZn) were used in this initial study. Zn sources were used since we have studied the photochemistry of these compounds for some time and are quite familiar with the deposition process using 257-nm radiation. We note here that our choice of Zn for this feasibility study in no way precludes the use of other organometallic sources involving Al, Mo or W for actual application in an industrial setting.

Photochemical depositions of repair structures are accomplished by focusing the 257-nm beam from a frequency-doubled, argon-ion laser tuned to 514 nm onto a sample mounted in a stainless-steel cell containing DMZn or DEZn gas. The incident ultraviolet beam will photodissociate molecules in the gas-phase and in the adlayers. Since our interest is in maskless direct writing of micrometer structures, it is important to enhance the adlayer component of the deposition and suppress the gas-phase component, which is less spatially restricted. Some control over the relative contributions of the two components is achieved through manipulation of ambient temperature and laser spot size. While the adlayer thickness increases with lower

temperatures, room temperature is a convenient ambient temperature yielding sufficient adlayer coverage.

The solution of the problem of step coverage for repair of packaging structures is shown in Fig. 2(a) and 2(b), where DEZn and DMZn are the organometallic sources, respectively. Note that this step coverage was accomplished on undercut Cu lines rather than actual breaks of irreproducible, though more easily addressed, geometries. Figures 2(c) and 2(d) show successful connection of two Cu lines and the corresponding I-V characteristic. The resistivity of the line is within a factor of three of the bulk resistivity of Zn metal, which is more than adequate for a satisfactory repair. A major problem in repairing package defects is to account for the large discontinuity in step height at the break.

### III. Laser Processing of GaAs

#### A. Laser Direct Writing on GaAs

The low-temperature treatment available using laser processing is important, for example, in the processing of compound semiconductors which often contain a volatile component. In this report, we discuss room-temperature laser deposition of Zn on GaAs substrates. Both Zn and GaAs are materials which are sensitive to processing conditions. The high vapor pressure of Zn makes it unsuitable for use in high vacuum systems, and the loss of arsenic during thermal processing of GaAs is a well established problem. Here, good quality conductive Zn lines were written on GaAs and used as wiring for laser-written devices. In addition, large-area excimer-laser-deposited Zn/GaAs Schottky contacts were investigated. Finally, the ability of laser irradiation to modify the Zn/GaAs interface during the deposition process was examined. Zinc was chosen in order to study its inadvertent interdiffusion into GaAs which can occur during low-temperature photometallization.

Photochemical deposition of micrometer structures is accomplished by focusing the 257-nm beam from a frequency-doubled, argon-ion laser, onto a GaAs sample mounted in a stainless-steel cell containing dimethylzinc gas (DMZn). The cell can be moved by computer-controlled stages with an accuracy of 0.25  $\mu\text{m}$ . The deposition conditions of 1.5 mW ultraviolet light, 10-Torr DMZn and about 2  $\mu\text{m}/\text{sec}$  sample translation speed were chosen to yield optimal spatial resolution. SEM images reveal well defined lines which contain particles with characteristic dimension  $\sim 0.15 \mu\text{m}$ . The resistivity of deposited metal is a reliable measure of both material

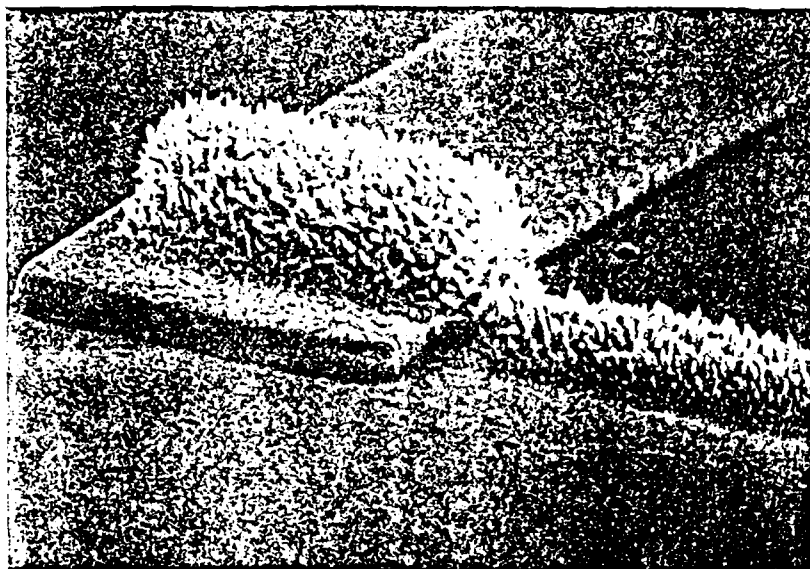


Fig. 2a. Successful step coverage using laser-deposited Zn from 10 Torr of DEZn.

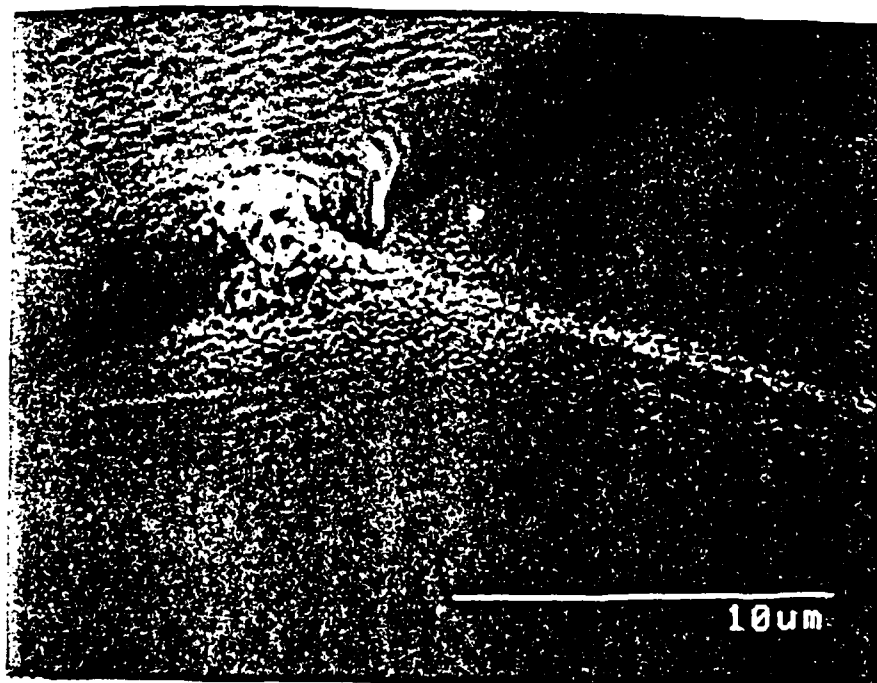


Fig. 2b. Successful step coverage using laser-deposited Zn from 10 Torr of DMZn.

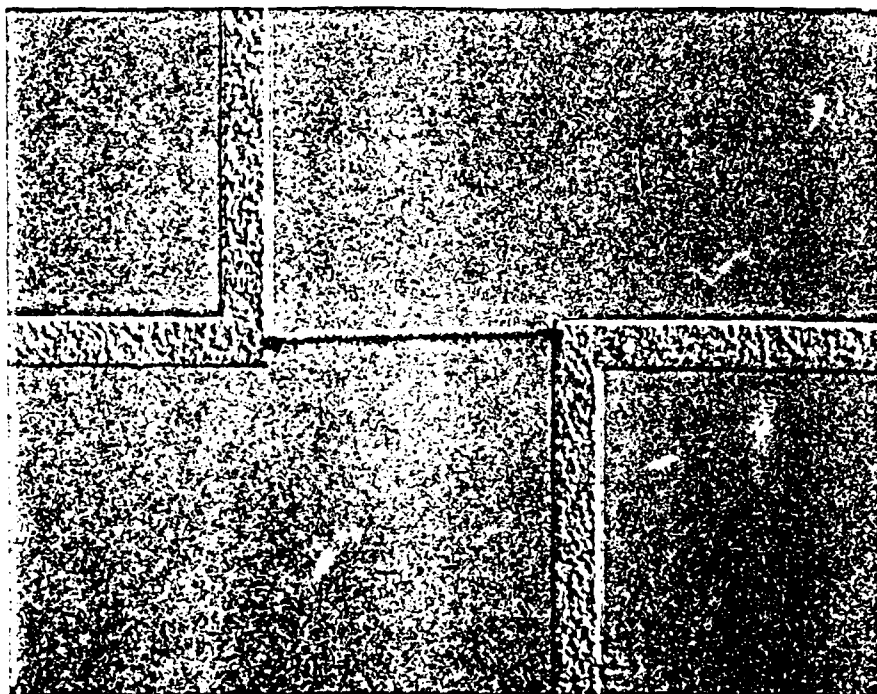


Fig. 2c. Laser written interconnect between two pre-existing Cu lines of wafer-scale Cu/polyimide package. The magnification is 300x.

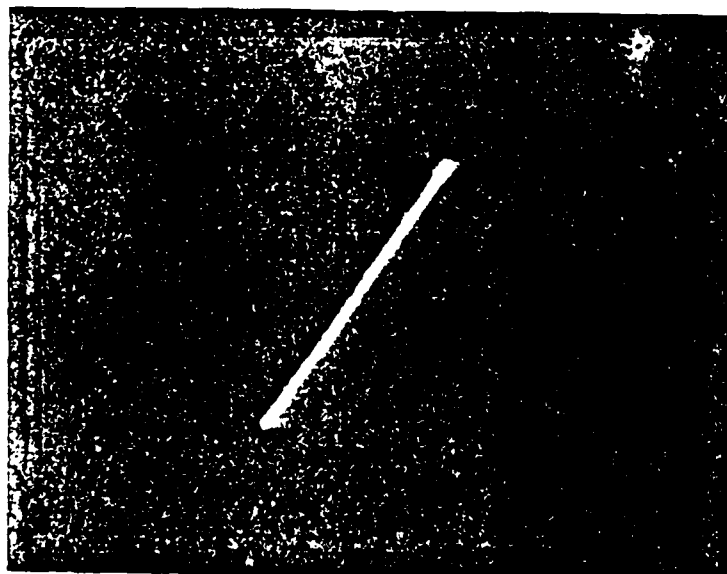


Fig. 2d. Current-voltage characteristics for the interconnect shown in Fig. 2c.

purity and microstructural integrity. Resistivity ratios between our deposits and the literature value for bulk Zn ( $6 \times 10^{-6} \Omega\text{-cm}$ ) are typically 7 for metal lines deposited with no thermal treatment. This compares well with results for other laser photodeposited metals cited in the literature, and is adequate for many customization applications.

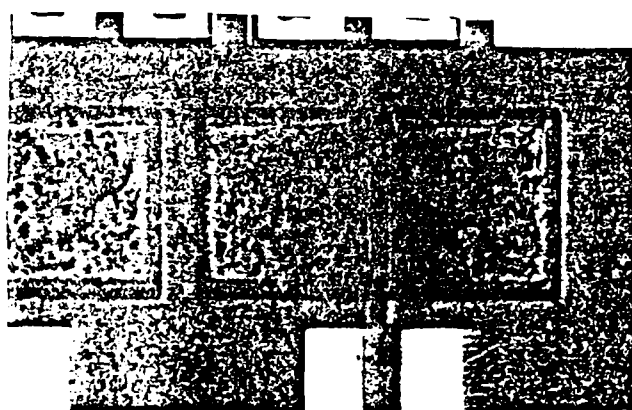
Both the control over deposition geometry and the stability of the contacts were evaluated by fabricating gates and interconnects for metal-semiconductor field effect transistor (MESFET) and charge-coupled device (CCD) integrated circuits. In addition, these experiments were used to demonstrate how the flexibility inherent in laser deposition makes it useful during the design process, since gates of different widths and thicknesses can be fabricated either in the center of channels or to one side if desired, as shown in Figure 3a. The MESFETs were fabricated on  $1.0 \times 10^{16}/\text{cm}^3$ , n-type epitaxial GaAs mesas on semi-insulating GaAs. I-V characteristics of the device are shown in Figure 3b. Measured transconductances for the laser-formed MESFETs range from 15 to 25 mS/mm. Pinch-off occurs at  $\sim 7\text{V}$  and the breakdown voltage is  $\sim 9\text{V}$ . These transconductance values are low since the substrates were optimized for CCD rather than MESFET applications. The same transconductances were obtained for MESFETs fabricated with evaporated aluminum gates through conventional photolithographic processing. Finally, the laser-deposited lines showed good step coverage over the  $45^\circ$ ,  $1.3\text{-}\mu\text{m}$  high mesas. In fact, an advantage to the laser deposition technique is that good step coverage is obtained even for more abrupt steps.

#### B) Applications of CW-laser Processing to GaAs Device Technology

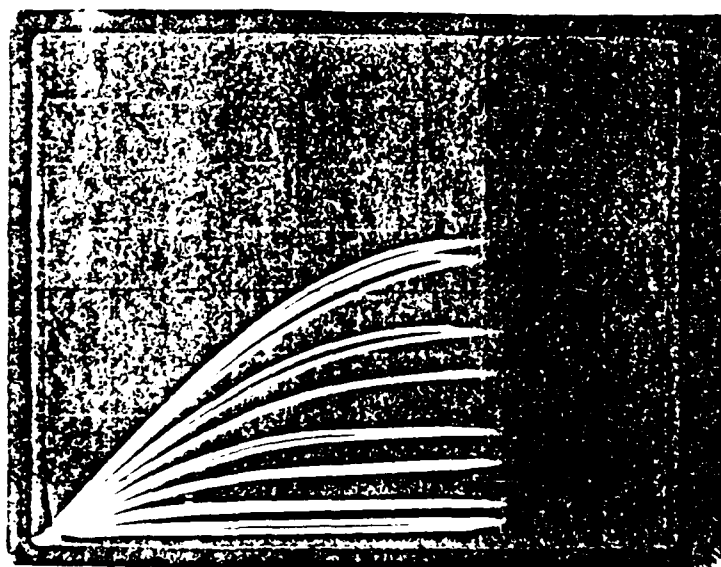
##### - CW Laser Doping of Micrometer-Sized Features in GaAs Using a Dimethylzinc Ambient

We have examined the characterization and utilization of a new cw process to laser-direct-write shallow-doped microstructures on GaAs and InP substrates. This capability is desirable for such applications as tailored modulation of Schottky-barrier height, ultra-shallow doping for VLSI applications, and local disordering of multiple-quantum-well structures for optoelectronic applications. Our CW laser-based doping process has the capability to fabricate shallow doping profiles and laterally-varied doping profiles with minimum impact on preexisting device structures. In this single-step process, a 514-nm beam from an  $\text{Ar}^+$  laser focused to  $2.5 \mu\text{m}$  produces a temperature rise of  $\sim 500\text{-}700^\circ\text{C}$  confined to a micron-sized region of a GaAs substrate. Ambient dimethylzinc (DMZn) molecules dissociate at the heated spot and solid-state diffusion of Zn atoms results in local doping of the GaAs. As shown in Fig. 4, secondary-ion

## GaAs MESFET WITH A LASER DEPOSITED Zn GATE



(Fig. 3a)

100  $\mu\text{m}$ 2 mA  
DIV

1 V/STEP

Fig. 3b

1 V/DIV

Fig. 3: (a) Photograph of a MESFET with a laser-deposited Zn gate. In order to customize the circuit and define the source and drain electrodes, the gate is positioned to one side of the channel. (b) I-V characteristics for the MESFET shown in (a). The looping is due to the properties of the substrate used.

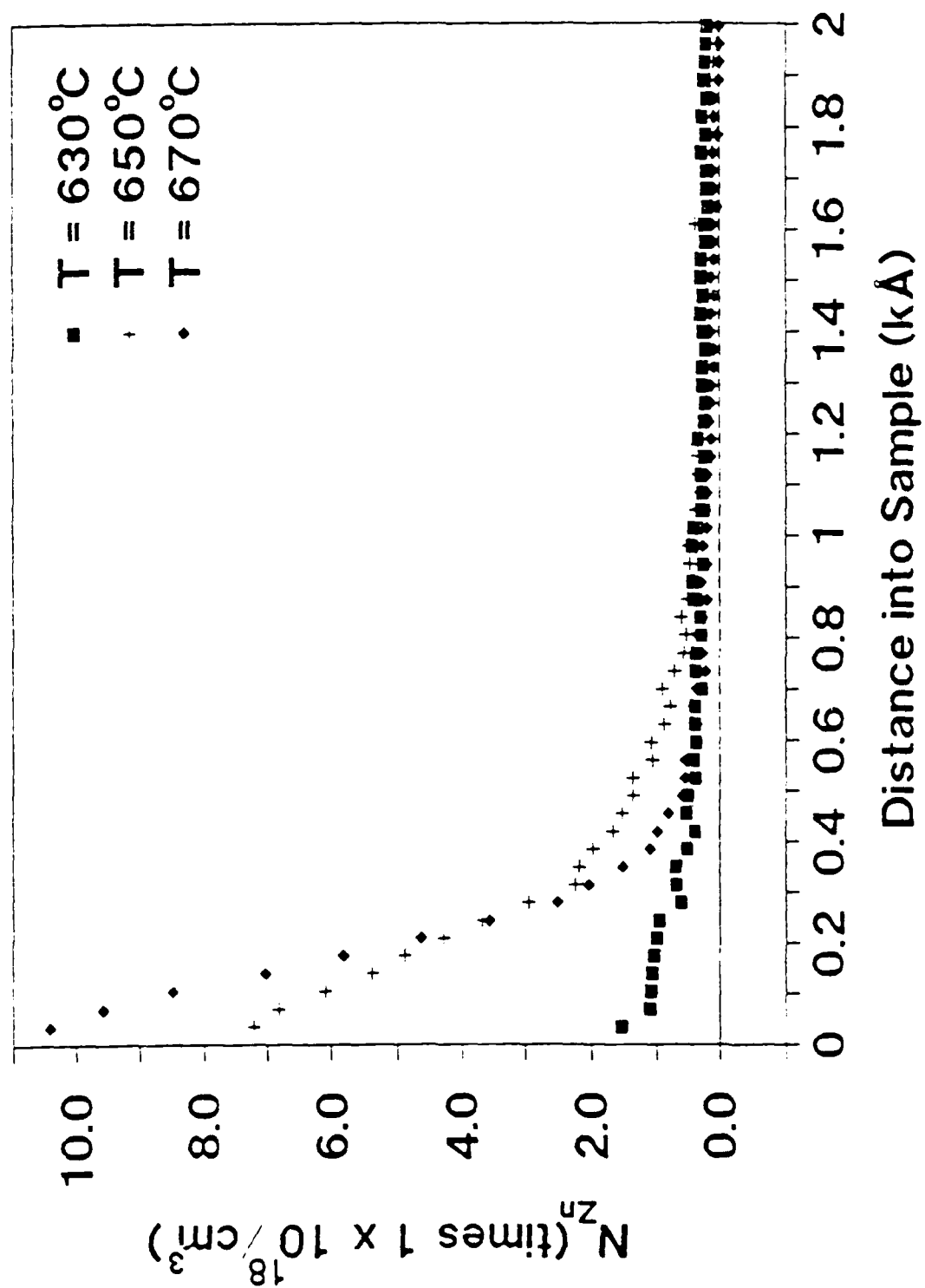
mass spectroscopy done with Steven Schwarz of Bellcore in Red Bank, NJ has shown that Zn dopant concentrations of up to  $1 \times 10^{19}/\text{cm}^3$  can be distributed over ultimate depths of from 100-500 Å. Raman microprobe spectroscopy done with Hua Tang and Prof. I. Herman at Columbia University has corroborated the SIMS measurements and shown that the lateral extent of the laser-doped features is significantly narrower than the width of the processing laser beam (Fig. 5). In a preliminary measurement of electrical activation, Al contacts to n-GaAs have been modified using the process. Factors limiting the process window have been identified. In particular, a new gas-phase etching effect has been identified and is currently being studied (below).

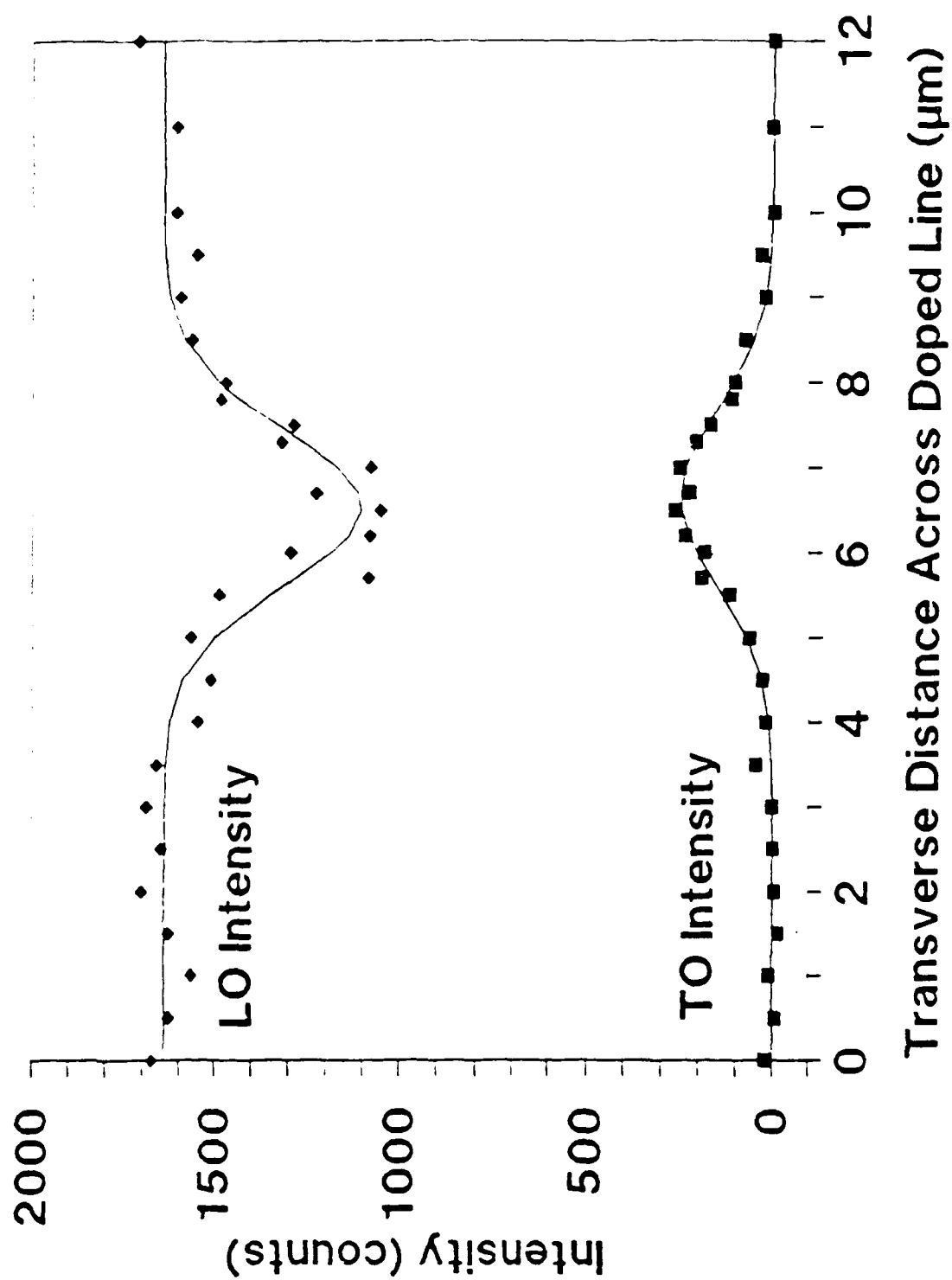
### C) Laser Controlled Modification of Electrical Properties of GaAs Surfaces

In contrast to the fact that the clean vacuum/GaAs (110) interface, obtained by cleaving in ultrahigh vacuum, is free of surface states in the energy gap, real air/GaAs and insulator/GaAs interfaces resulting from wet or dry etching or from various insulation processes, generally possess a high density of surface states which tend to fix the position of the surface Fermi level within a certain narrow range in the energy gap. At present, no reliable technology exists which can reduce the surface-state density down to a level which is acceptable for device fabrication. Alteration of the interface chemistry, however, can result in large variations in Schottky barrier heights for metal/GaAs contacts. We have shown that when metal was deposited on GaAs which has been oxidized by using 248-nm illumination to enhance the formation of a thin oxide layer, the Schottky barrier for the contact varies much more strongly with the work function of the metal overlayer than for contacts to clean GaAs surfaces.

The MESFET (Fig. 6) and diode (Fig. 7) structures chosen to characterize these laser-oxidized surfaces were fabricated using Au/Ge/Ni metallization on a Si-doped n-type epilayer ( $10^{17}/\text{cm}^2$ , 1-mm thick) grown by MOCVD on a semi-insulating (100) substrate. To fabricate these devices, a pattern was defined in photoresist on the GaAs surface. Prior to loading into vacuum system, the samples were etched in  $\text{HN}_3\text{OH}:\text{H}_2\text{O}=1:2$  and blown dry with dry  $\text{N}_2$ . A detailed description of the following oxidation and Schottky metallization is presented in our previous reports and it will be avoided here.

Room-temperature current-voltage measurements were performed on all MESFET's and diodes to evaluate the results of the laser treatment. It was found that the transistor characteristics remained unchanged for irradiated and nonirradiated (control) samples. However,





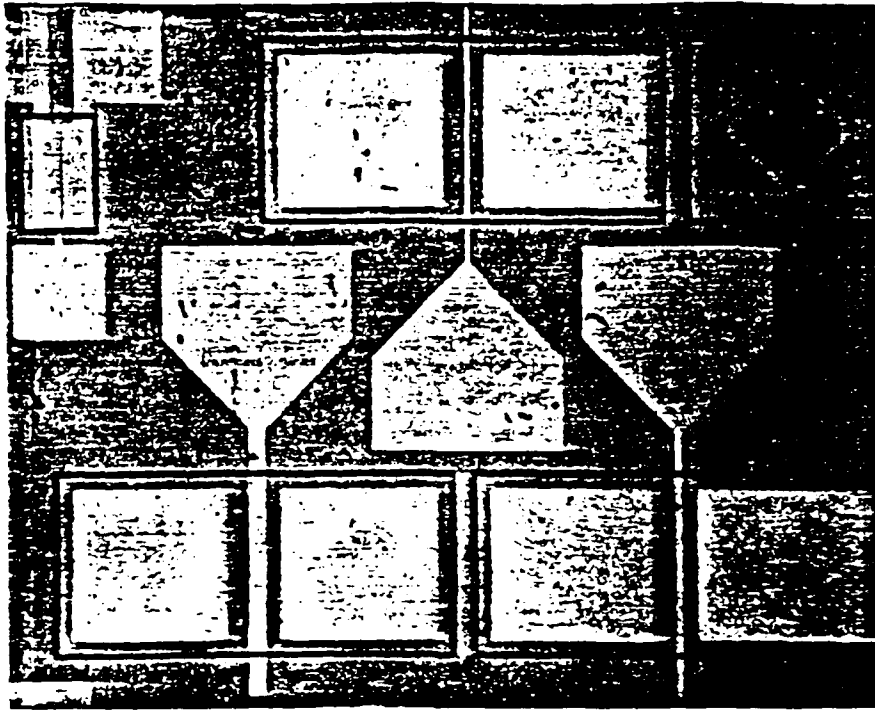


Fig. 6

The MESFET structures with laser-modified Ti Gates.

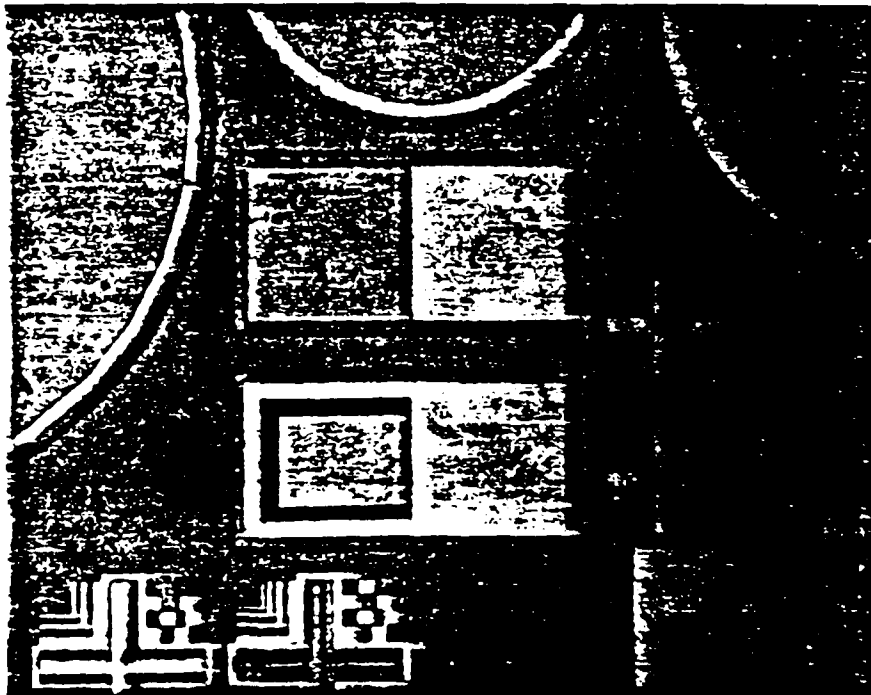


Fig. 7

The Schottky diodes with laser-modified Ti contacts.

the Schottky barrier height on all contacts was reduced as predicted by earlier experiments on samples, which were not lithographically processed. These preliminary results show that the laser-controlled modification of metal/GaAs contacts is a possible tool for systematic adjustment of the effective barrier height and may be of practical use in optimization of MESFET's and other devices. It is important to note that these laser treatments are done at fluences well below any material damage threshold and, for example, are possible in the presence of intact photoresists.

#### D. CW Laser Etching of Micrometer-sized Features in GaAs Using a Dimethylzinc Ambient

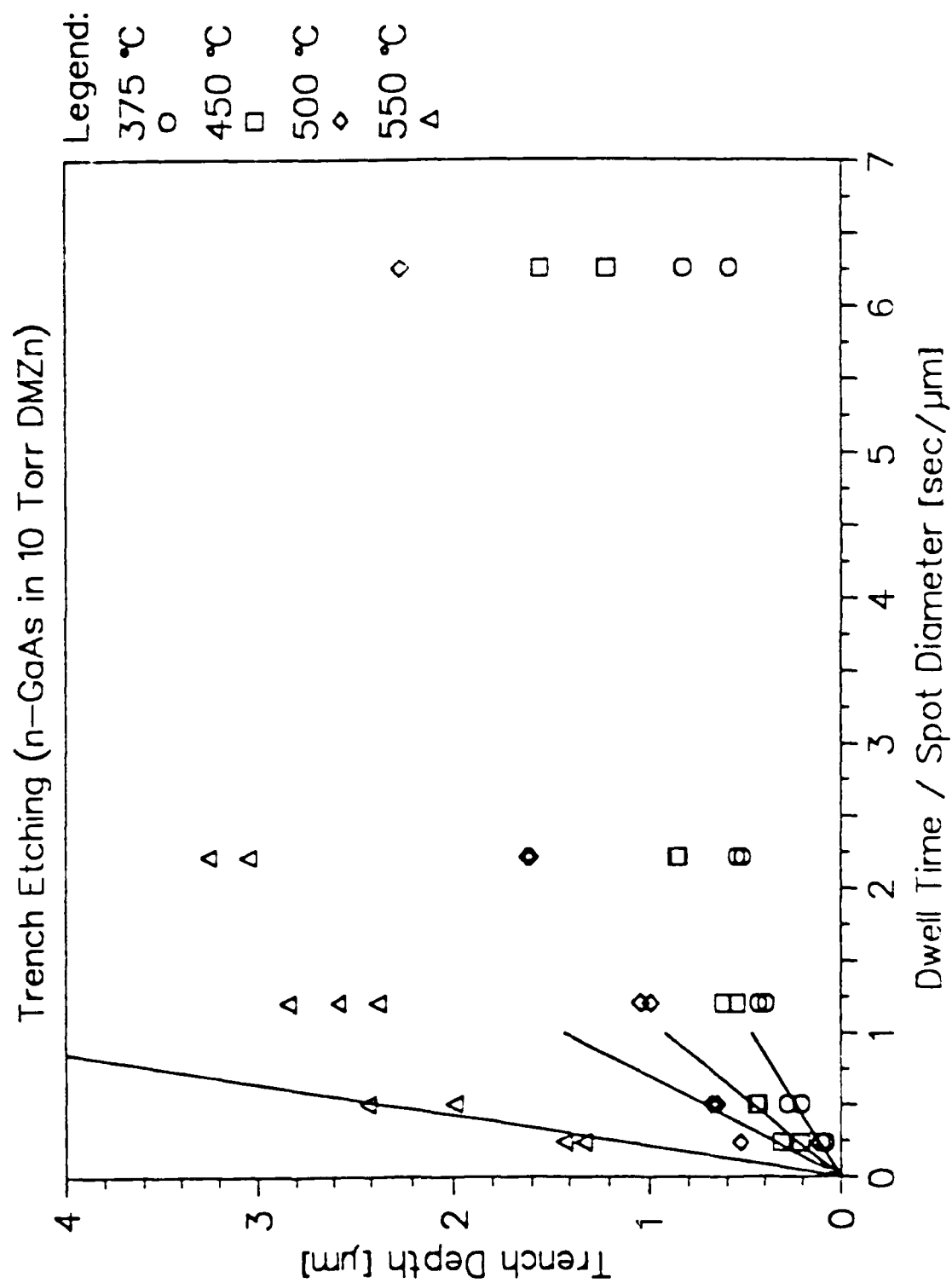
We have determined that a novel high aspect etching occurs when high concentrations of methyl groups from the dissociation of organometallic gases are generated in close proximity to a III-V semiconductor surface. This effect is minimized in the aforementioned doping experiments by using low pressures ( $\sim 0.01$  Torr) and short laser dwell times ( $\sim 1/20$  sec). The etching can be maximized by using higher DMZn pressures ( $\sim 10$  Torr) and longer laser dwell times ( $\sim 1$  sec). Under these conditions, the effect becomes a viable MOCVD/MOMBE compatible process for the direct-writing of surface-relief features on III-V substrates.

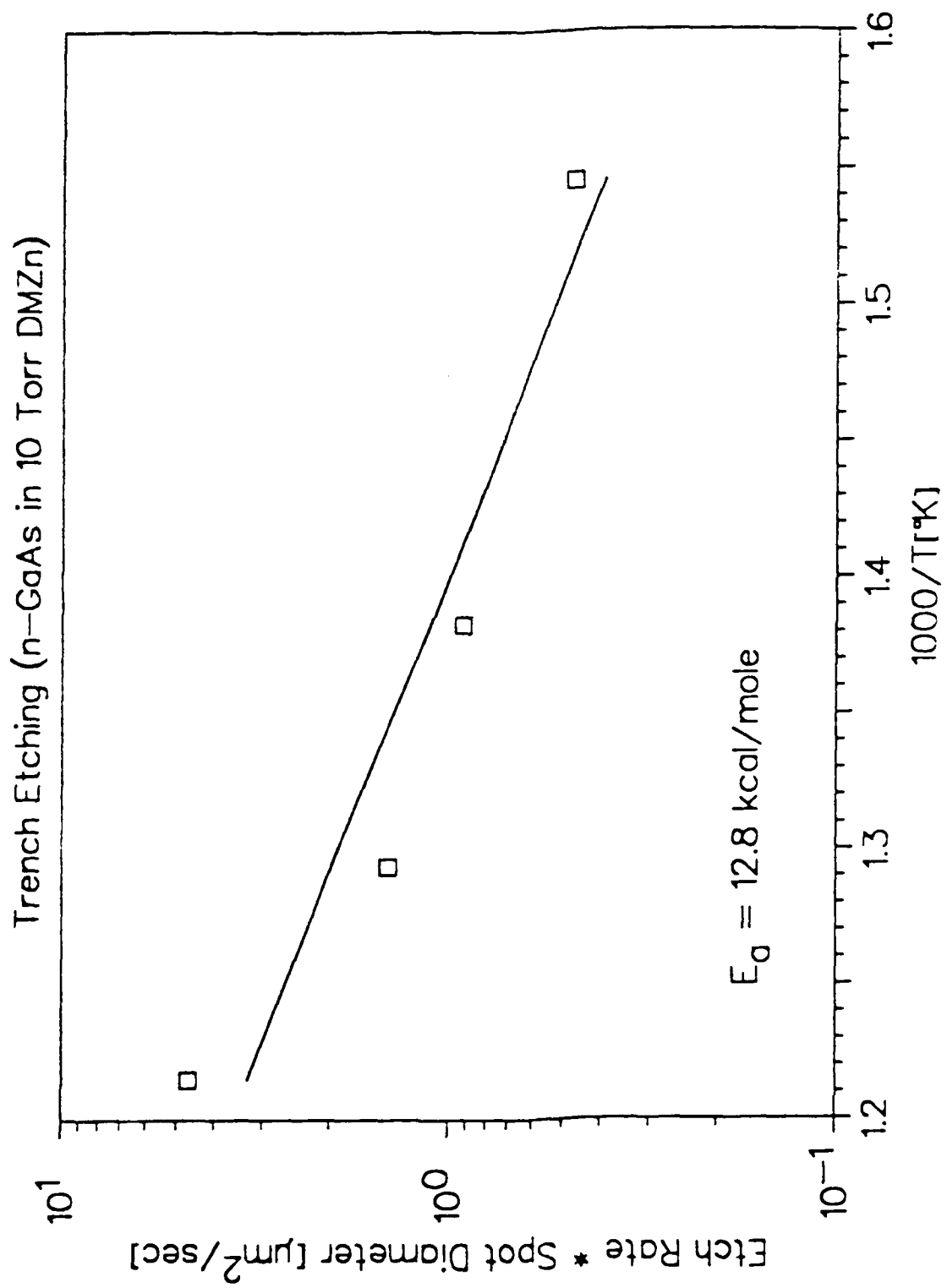
As shown in Fig. 8, etch rates for the process have been characterized in terms of laser-induced temperature and laser dwell time. Based on this data, the activation energy for the process has been calculated as shown in Fig. 9. Finally, the dependence of the etch rate on DMZn pressure (Fig. 10) has been investigated using *in situ* analysis of the reflected laser intensity and the parameter space for the successful avoidance of competing processes has been determined.

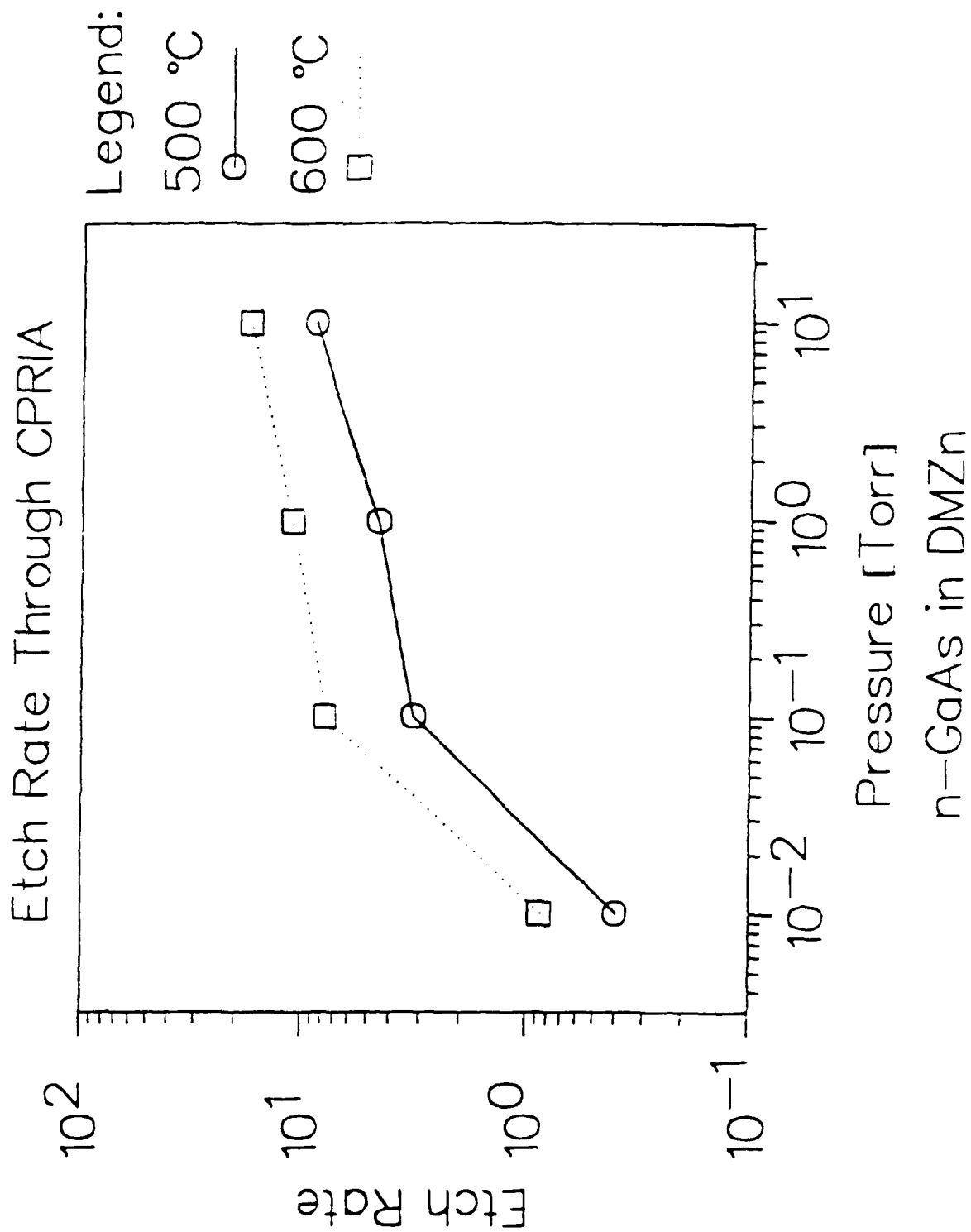
#### IV. Laser Writing of Integrated Optical Components

In this project we have concentrated our efforts on writing integrated-optical devices which will be of use for optical processing or optical-data transmission. Thus far our experiments have involved the fabrication and the investigation of waveguide and grating structures in InP and GaAs.

The first device structure which we have designed and tested has been a GaAs waveguide in an epitaxial layer on AlGaAs. The structure will be created by etching two parallel grooves in the GaAs sample with UV or green light in an aqueous solution. Note that the computer-controlled writing of waveguides allowed real-time adjustment in the width during fabrication







for spatially mode-selective waveguides. Furthermore, a variation in the thickness of the guide (tapered waveguide) has been produced when the waveguide is created in the top layer. This laser-etching technique has allowed the ready customization of the waveguide's horizontal position on the substrate. The connection to a hybrid electrooptic structure using fibers or an underlying waveguide have also been accomplished.

Note also that a sharper physical insight into the light-guided etching has been a major result of our work on characterization of the process. Work in this area has emphasized electromagnetic modeling of the waveguides using novel mathematical techniques. In addition, the physics of ultrasmall scale photoelectrochemistry have been examined.

#### A. Optically Induced Deep Periodic Structures on Semiconductor Surfaces

Increasing applications are being found for lasers and optical techniques in the fabrication of semiconductor devices. For example, by using two interfering laser beams to initiate localized chemical reactions, spatially periodic structures can be produced on semiconductor surfaces. Practically, such holographic structures are of interest because of their potential for utility in a variety of electrooptical and electronic applications.

Most of our initial work on holographic processing has emphasized high-resolution gratings. It was shown that light-sensitive aqueous etching of semiconductors in conjunction with coherent laser radiation provides a simple method for recording the gratings.

An important new result of our laser-controlled etching experiments was fabrication of arrays of deep, submicrometer-size grooves in GaAs crystals. Such grating can be obtained by projecting an interference light pattern. Namely, two ultraviolet laser beams were symmetrically incident onto a GaAs sample surface where they intersect at a small angle. The interference fringe pattern produced by the intersecting beams results in a sinusoidal variation in the irradiance at the sample surface with the fringe spacing of  $\sim 1.4 \mu\text{m}$ . In contrast to the results described previously, the long-exposure etching, typically 30 to 40 minutes, results in deep, vertical features. A scanning electron micrograph of the cross-sectional profile of 20- $\mu\text{m}$ -deep grooves is shown in Fig. 11.

The entrance edge of the etched structure is tapered for a short distance into the sample, i.e.  $< 1 \mu\text{m}$ , corresponding to the incident, sinusoidal laser intensity pattern. However, for deeper etching, the grooves assume a characteristic vertical shape as the feature sidewalls become vertical. The etched width,  $\sim 0.5 \mu\text{m}$ , remains then constant, independent of the etched depth.

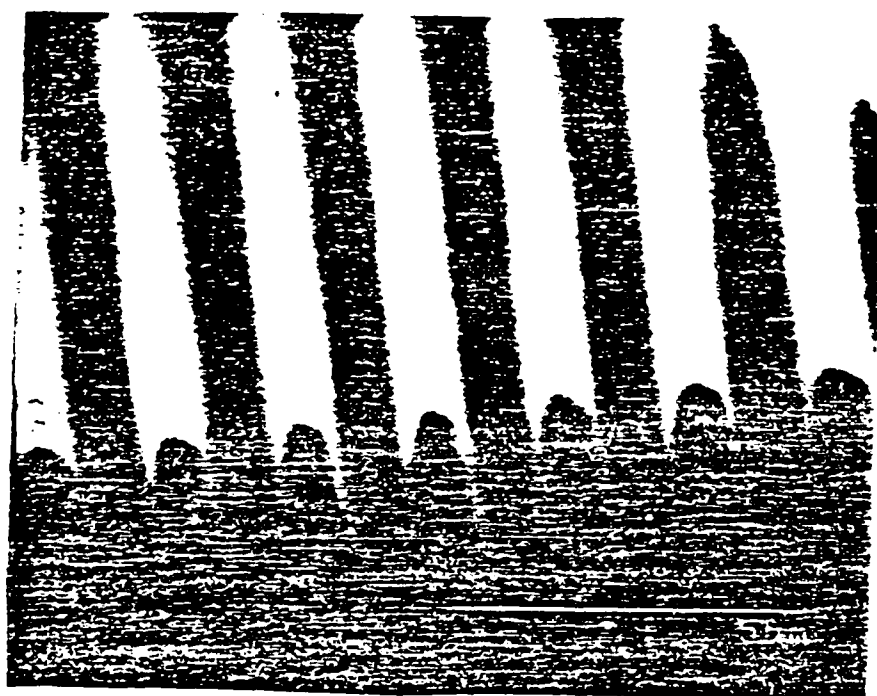
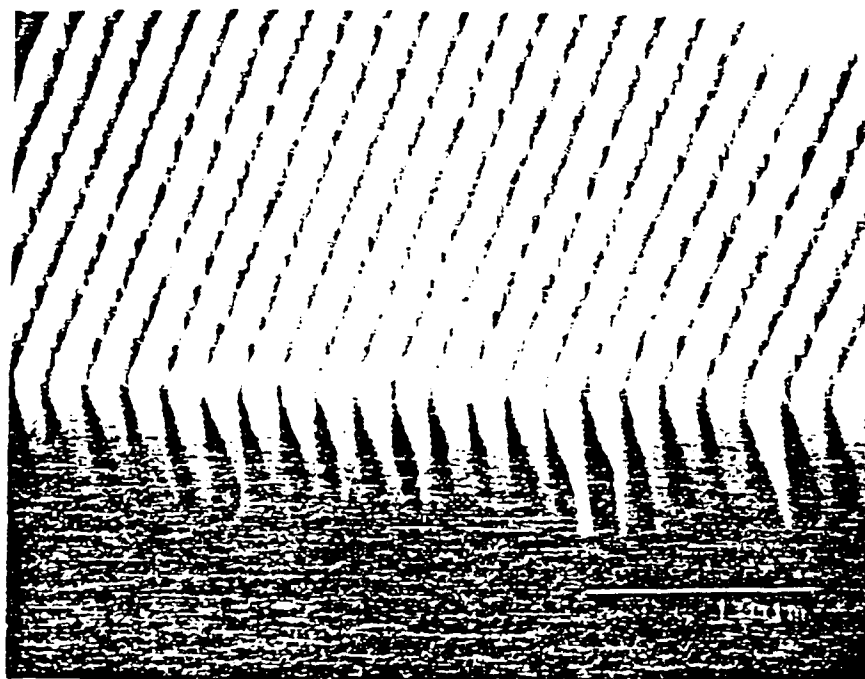


Fig.11. SEM micrograph of the cross-sectional profile of deep grooves etched in GaAs.

The etched structure acts now as a self-propagating, hollow waveguide which confines and efficiently transmits the processing laser light.

In order to support our optical device work, we have now characterized the development and spacing dependence of deep gratings. The etched structure was measured with both optical methods and scanning electron microscopy. An important feature of the direct etching process is that the parameters of the gratings can be monitored during fabrication. The processing laser beam, reflected from the etched corrugation, produces a diffraction pattern that characterized the depth and the shape of the grating profile at any given moment.

In order to perform *in situ* monitoring, the diffracted, first-order beam was measured with a commercial power meter. Theoretical treatments of a simple sinusoidal grating have shown that the ratio of the minus-first-order diffracted and the incident reflected  $I_0$  (taken as 100%) determines the depth of the grating grooves. For shallow gratings, the grating growth rate can be determined to within an accuracy better than 10% from the position of the first maximum of a Bessel function. Deep gratings, e.g.  $> 5 \mu\text{m}$ , and detailed groove profiles were measured with a scanning electron microscope and compared with the optical measurements.

#### B. GaAs Detector Structure for Vertically Coupled Fiber Optic Interconnects

Optical interconnection of high-speed integrated circuits has shown potential for increasing overall interchip communication bandwidths. In general, fiber-optic waveguides provide the most practical and versatile transmission medium for optical signals. Full realization of the potential benefits of fiber interconnects requires the development of techniques for coupling many fibers to a single IC chip; each individual connection should occupy a minimum amount of real estate.

The device work on this technique has been supported by a separate DARPA contract to Columbia. The principal investigators are Professors Prucnal and Fossum. The supporting work on laser etching has been pursued in this DARPA/AFOSR contract.

Previously, we have developed one such technique, based on the vertical insertion of a tapered optical fiber into a laser-etched cavity situated on the front surface of the silicon receiver chip. Photodetectors fabricated by doping the cavity interior to form a p-n junction diode exhibited good dark current and responsivity characteristics, but a modulation bandwidth below 10 MHz. One way to improve the bandwidth is to implement a backside-illuminated detector structure. Schematic cross-sections of both frontside and backside coupling structures are shown

in Fig. 12.

The backside integrated fiber optic coupler (IFOC) depicted in Fig. 1(b) is fabricated in GaAs, on a semi-insulating substrate with an n-type (Si,  $N_D = 1.0 \times 10^{16} \text{ cm}^{-3}$ ) epitaxial layer grown by MOCVD. A Schottky photodiode formed by Al evaporation is used as a photodetector, to maintain compatibility with the processing of LSI GaAs logic circuitry. Amplification and multiplexing/demultiplexing circuits based on depletion-mode GaAs MESFETs are integrated with the IFOC detectors. The photodiodes and transistor gates are deposited in the same evaporation step. The detector area need not be much larger than  $100 \mu\text{m}^2$ , corresponding to the core of a single-mode fiber, while the majority of the overall fiber footprint can be devoted to photoreceiver front-end circuitry. We have fabricated a source-follower configured diode-transistor pair in which the MESFET encircling the photodiode lies entirely within the fiber footprint. A photograph of the circuit appears in Fig. 13.

Fabrication of the backside-illuminated device involves vertical insertion of an optical fiber into a cylindrical cavity formed by a combination of conventional etching processes and the laser enhanced photochemical etching process described in our earlier reports. In this structure the constraints on the cavity dimensions are more stringent than in the case of the frontside IFOC. The coupling cavity rises vertically from the backside of the wafer through the semi-insulating substrate and into the  $2.0\text{-}\mu\text{m}$  thick epitaxial layer. Proper alignment of the front-surface photodiode and the cavity site on the back surface is ensured by performing photolithography on a system equipped with an infrared video camera and monitor.

### C. Characterization of Laser-Fabricated Waveguides

In general, rib waveguides confine the optical field in both the vertical and horizontal directions. In a GaAs/AlGaAs heterostructure, light is vertically confined within the GaAs layer which is surrounded on top by air and on the bottom by AlGaAs. Horizontal confinement of the wave is achieved in conventional rib structures by etching a mesa which introduces a discontinuity in the horizontal effective index of refraction in the GaAs layer, the thinner region having a lower effective index of refraction shown in Fig. 14(a). We achieved the same effect by laser etching two trenches separated by the distance of the width of the guide. These trenches locally reduce the effective index of refraction, which laterally confines the wave to the central region as shown schematically in Fig. 14(b).

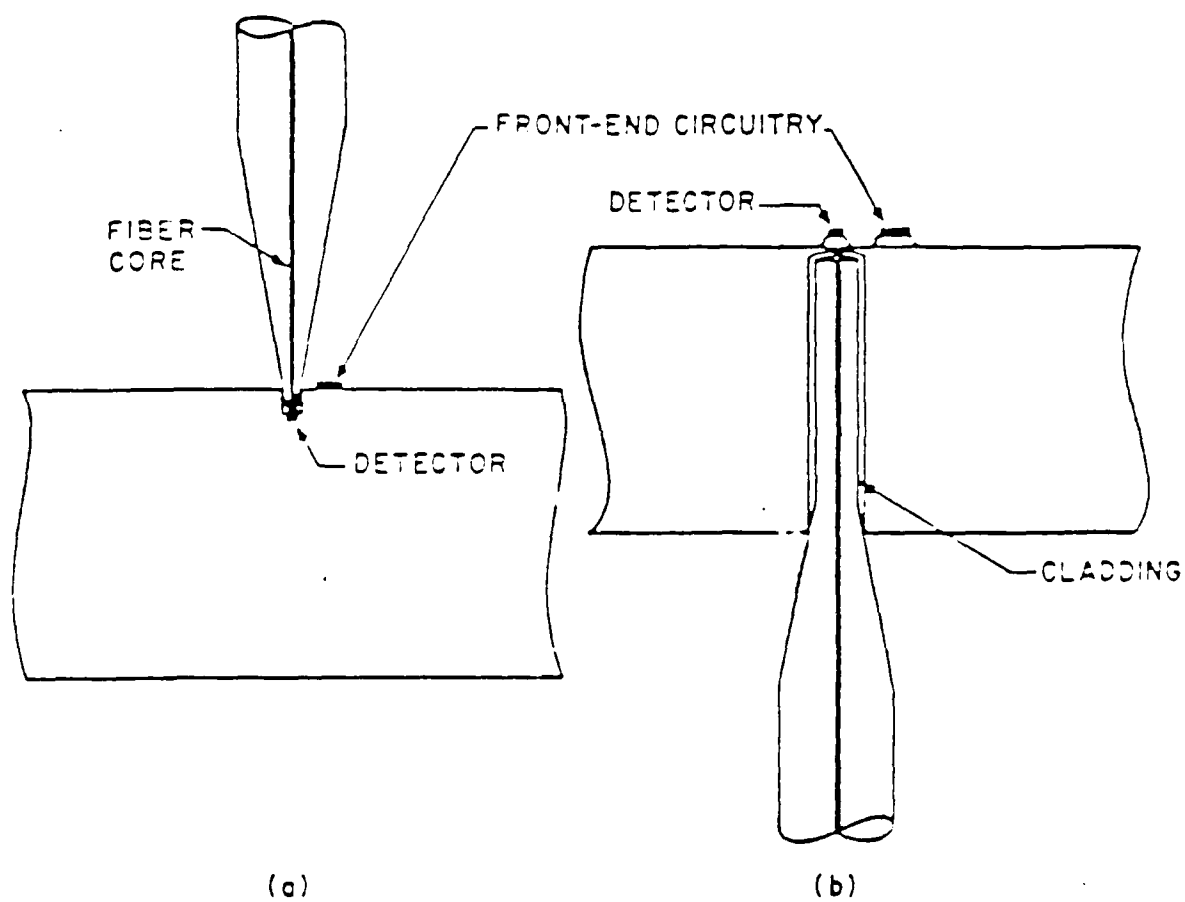


Fig.12. Schematic cross-section of

- (a) previously reported frontside integrated fiber optic coupler (IFOC) structure, and
- (b) backside structure designed for faster response and reduced crosstalk

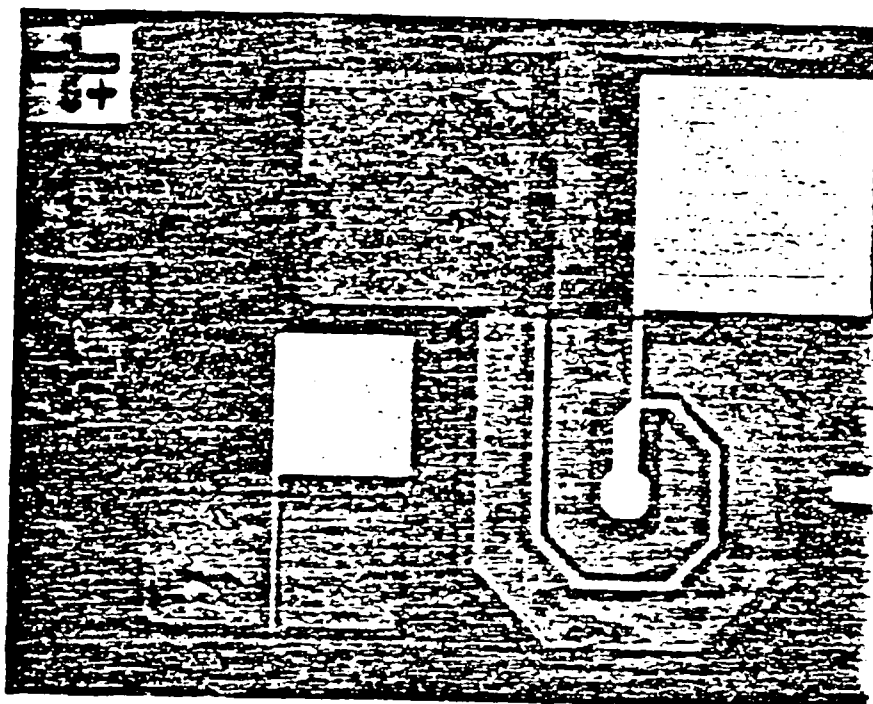
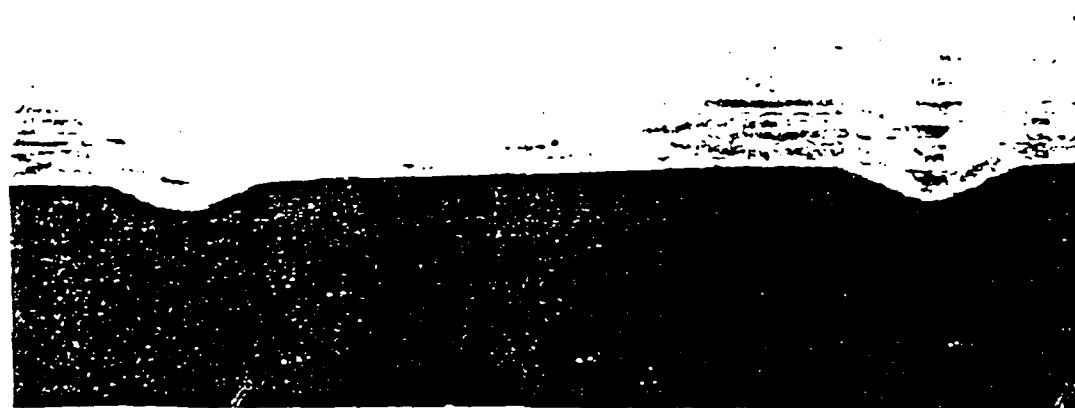


Fig. 13. Photograph of detector photodiode surrounded by a source-follower MESFET amplifier which lies within the footprint of the input fiber.



(a) 10  $\mu\text{m}$



(b)

Fig. 14.

(a) Cross-section of a rib waveguide formed by two trenches etched 1 $\mu\text{m}$  deep and 15 $\mu\text{m}$  apart. (b) Near-field optical output of a launched wave being confined to the region between the etched trenches [not to the same scale as (a)].

As we have reported previously, the test structure used to fabricate these guides is a four-layer heterostructure on an  $n^+$ -GaAs substrate. The 2- $\mu\text{m}$ -thick layers are from the top GaAs,  $\text{Al}_{0.3}\text{Ga}_{0.7}\text{As}$ , GaAs, and  $\text{Al}_{0.3}\text{Ga}_{0.7}\text{As}$  doped to  $n \approx 10^{16} \text{ cm}^{-3}$ . Most of the etching was confined to the top GaAs layer to form a single-layer rib waveguide using the underlying AlGaAs layer as the cladding. A schematic cross section of an etched waveguide is shown in the inset of Fig. 15(b). Two trenches were etched  $\sim 20\text{-}\mu\text{m}$  apart and 1- $\mu\text{m}$  deep in the 2- $\mu\text{m}$ -thick top GaAs layer. This process lowers the effective index of refraction in the region of the trenches enough to confine the wave to the central region.

The performance of this etched structure can be seen in Fig. 15, which shows the measured efficiency of optical transmission as a function of the etched trench depth,  $d$ . For shallower trenches the waveguide output decreases with  $d$  since a significant amount of light is radiated into side regions as shown in Fig. 16(a). This loss mechanism is not present in conventional rib waveguides. For trenches etched deeper than  $\sim 0.5 \mu\text{m}$ , the output power from the guide does not vary significantly with  $d$  as shown in Fig. 16(b). In particular, since the trenches have finite width, light can leak through the narrow region under the trenches and radiate into the side regions. This loss is a function of both trench depth,  $d$ , and width,  $w_t$ . Note that the loss curve flattens out in Fig. 2 for  $d \approx 0.5 \mu\text{m}$ , in the regime where the radiation loss becomes negligible.

#### D. Laser Fabricated Directional Couplers and Two-Level

A major advantage for the use of laser etching in forming optoelectronic structures is the ability to vary the depth of etched features smoothly across the surface of the wafer. This variation is accomplished by changing the power of the incident laser beam. This depth variation provides control over the lateral effective index as shown in Fig. 17. We have recently utilized this capability to fabricate a waveguide coupler, which is far more compact than the usual directional coupler designs, since it allows the two waveguides to run proximate to each other across the wafer surface. Conventionally, such couplers are made by bringing two fixed-index waveguides into close proximity to permit coupling over a specific length. In our coupler, the coupling region is defined by a local reduction in the depth of one of the confining trenches and not only by the proximity of the waveguides. The coupling region can be smoothly enclosed by a gradual transition in trench depth, thus minimizing the excitation of higher order modes or back reflections. Figure 18(a) shows a schematic of the laser etched coupler. The device has 10- $\mu\text{m}$ -

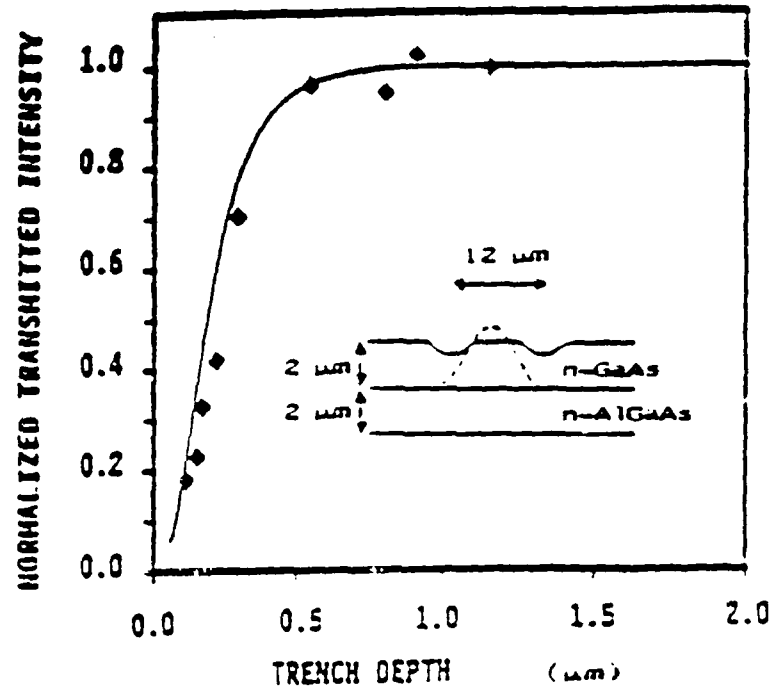


Fig. 15. Measurement of the normalized transmitted light intensity versus trench depth in a 12-μm-wide guide. The calculated transmitted intensity is plotted as a solid line.

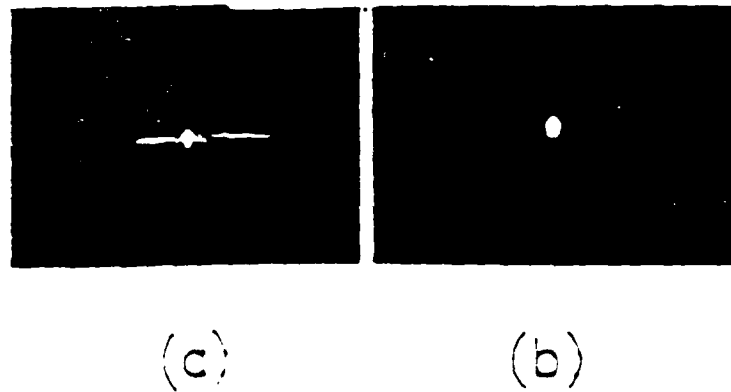


Fig. 16. Photographs of the optical output image for a waveguide defined by (a) shallow (0.2-μm-deep) and (b) deep (0.6-μm-deep) trenches.

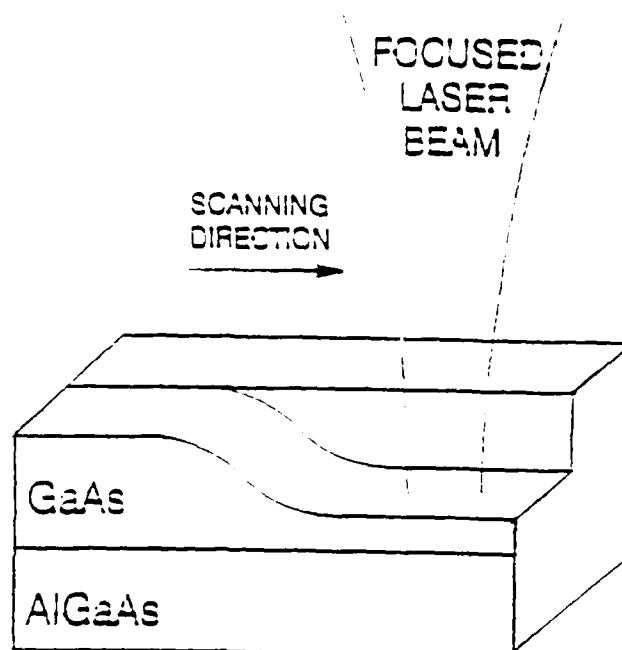


Figure 17. Schematic diagram illustrating the concept of grading effective index through changing the etch depth. Control of the etch depth is provided by varying the laser intensity or the scanning speed of the computer-controlled translation stage.

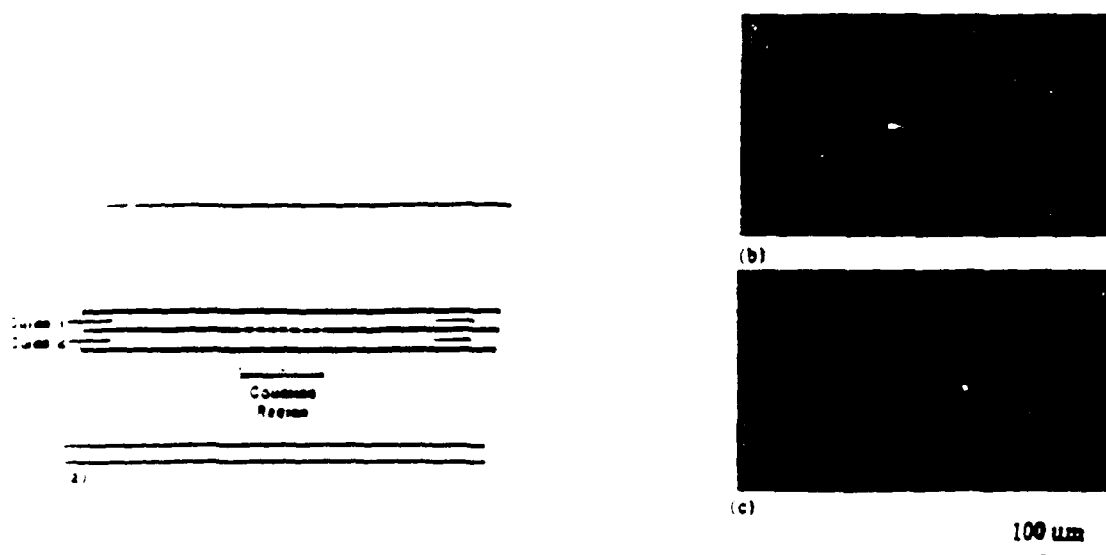


Figure 18 (a) Top-view of a directional coupler. A dashed line indicates a shallow trench (coupling region). Optical output of above coupler ( $L=1$  mm) for (b) wave launched into right guide, and (c) wave launched into left guide.

wide twin guiding regions. The main length of the structure consists of three trenches separated by identical guide widths. Efficient coupling occurs only in the region where the common central trench is shallow. Figures 18(b) and 18(c) show the coupler output (coupling length = 1 mm) of the two guides when the light was launched into the right guide and into the left one, respectively. In both cases, the guided wave is coupled into the adjacent guide.

Our laser etching technique has also allowed us to form multilevel waveguides in a single-step process. Such structures, even when formed in the same vertical plane, are important both for transmission of separate optical channels and for stacking passive and active devices. In the four-layer GaAs/AlGaAs structure used here, both the first and the third layers can guide light. We fabricated the two-level structure by laser etching deep trenches into the third layer thus confining a wave in both the first and third waveguiding layers. This single-step, two-level waveguide process significantly reduces the complexity and number of processing steps necessary to fabricate waveguiding structures in different planes.

#### E. Optical Fabrication of Integrated Optical Components - Y's and Bends

The need to direct light between components of an optical circuit requires waveguiding structures such as tapers, bends, and Y-branches. One of the unique features of micrometer-scale, laser-controlled etching is that any structure can be masklessly fabricated by simply programming the computer-controlled translation stage to move the sample below the fixed laser spot in any desired pattern. Thus, these passive waveguiding structures were easily micromachined on GaAs/AlGaAs material as shown in Fig. 19. Waveguiding bends with a width of  $20\text{ }\mu\text{m}$  were characterized over bend angles varying from  $0.5^\circ$  to  $4^\circ$  by considering the power ratio of the waveguide bend output to that of an adjacent straight waveguide. Both are excited with the same input power. However, since this structure contained two bends, the bend loss was determined by taking the square root of this power ratio. In the given range of bend angles, the losses ranged from 0.5 to 3.5 dB as shown in Fig. 20(a). Similarly, Y-branches with channel widths of  $20\text{ }\mu\text{m}$  and branching angles varying from  $0.5^\circ$  to  $0.4^\circ$  were characterized in the power splitting mode. The measured Y-branch transmission was determined by taking the ratio of the sum of output powers from the two output branches to that of a straight waveguide. The branch losses ranged from 0.9 to 1.5 dB over these branching angles as shown in Fig. 20(b). Note that the bend and branch losses seen here are comparable to similar structures lithographically fabricated using ion-beam assisted etching.

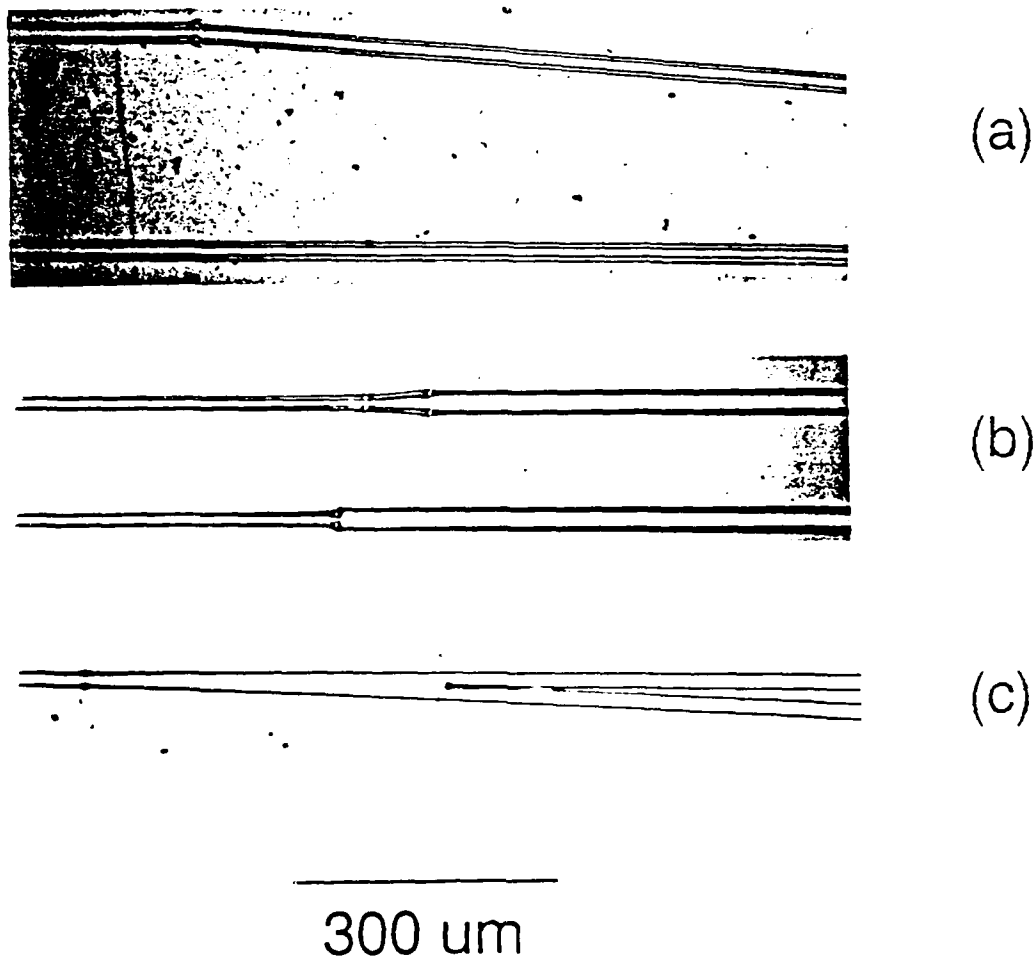


Fig. 19. Top view of masklessly fabricated waveguide (a) bends, (b) tapers, and (c) Y-branches.

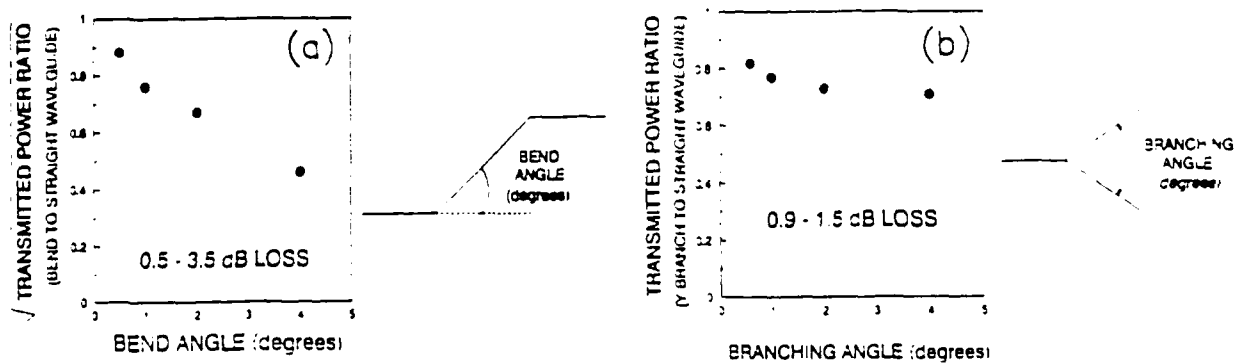


Fig. 20. Measured relative transmission through the laser-fabricated waveguide (a) bends and (b) Y-branches as a function of bend and branch angle, respectively.

#### F. Loss Reduction in Passive Waveguide Structures

A major advantage of laser etching optoelectronic structures is the ability to vary the depth of etched features smoothly across the surface of the wafer, which is very difficult to achieve lithographically. Experimentally, this is done by changing the intensity of the incident laser beam or by simply changing the etch time via the scanning speed of the computer-controlled translation stage. This provides an easy way for controlling the effective index within these waveguiding structures. Not only does the ability to grade the effective index open up the possibility for reducing the losses within waveguides transitions but also for generating new devices.

In addition, we have considered via theoretical analysis whether or not varying the effective index of refraction along a waveguide can be used to reduce losses in passive structures such as waveguide tapers, bends, branches and couplers. In this analysis, we considered a tapered rib waveguide as shown in Fig. 21(a,b) in which the etch depth of the lateral cladding region varies along the taper. We have used a local normal mode analysis to calculate the coupling coefficients and radiation losses in such structures. Preliminary numerical results indicate that in certain cases, an order of magnitude reduction in losses can be achieved by grading the effective index with in the taper. We are in the process of trying to understand these results and extend the analysis to other structures.

#### G. Laser Fabrication Technique to Forming Microcleaved Semiconductor Facets

Utilizing the varying optical and electrical properties of III-V layered materials provides many possibilities for novel fabrication techniques. Photochemical etching offers an important approach to the maskless processing of layered materials since it is sensitive to both the electrical and optical properties of the material. Here, we report on fabricating novel microstructures in GaAs/AlGaAs multilayered material by utilizing the confinement of photogenerated carriers to the alternating GaAs layers. Specifically, we apply this processing technique to forming microcleaved semiconductor facets.

One of the most interesting consequences of the unusual photocarrier-induced chemistry, as described in this report, is that it permits the formation of long material-selective undercuts. This microstructure has a number of immediate applications to integrated optics, including the cleaving of facets for mirrors in semiconductor diode lasers. In the monolithic integration of lasers with other optoelectronic components, a major drawback is the formation of laser mirrors

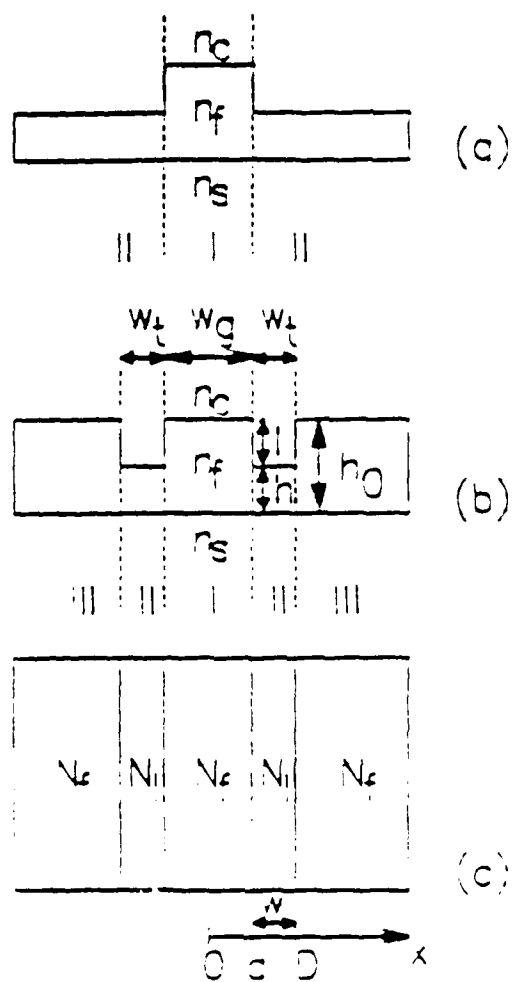


Figure 21. Sketch of (a) conventional rib waveguide, (b) laser fabricated riblike waveguide, and (c) effective slab waveguide corresponding to (b).

by the cleavage method which severely limits the size of the usable substrate area. To illustrate the potential use of this etching technique to the formation of laser facets in a two-step process, we have spent a considerable effort to develop a laser-etching technique to direct-write an "U"-shaped structure such that the legs of the "U" are spaced no more than twice the width of the undercut, i.e.,  $16\text{ }\mu\text{m}$ . This forms a cantilever since the sandwiched n-GaAs layer within the "U" is selectively etched away. By using a probe tip to apply mechanical pressure, we were able to microcleave the cantilever leaving behind a smooth semiconductor facet perpendicular to the surface without fracturing the wafer as shown in Fig. 22. Note that unlike the previously reported microcleaving method, we are able to work with low-Al-content AlGaAs.

#### H. Ultrafast Aqueous Etching of Gallium Arsenide

Laser-induced photochemical aqueous etching has previously been demonstrated in various types of semiconductors. This technique is a useful way to fabricate microstructures utilizing a well-controlled laser writing beam. The process is electrodeless, maskless, single-stepped, and produces damage-free structures in a non-thermal environment. However, the usefulness of this process to etch over large areas can be improved by increasing the speed of the etching. The process until now was slow for fabricating structures that would cover several hundred microns on a semiconductor wafer. However, we have now achieved an increase of over an order of magnitude in the etch rates of n-type GaAs. This process shows promise for micromachining on full, wafer-scale dimensions.

The etching experiments were primarily performed with the 257-nm output of a frequency-doubled, Ar-ion laser. In contrast to work previously reported using a nitric acid solution, n-GaAs was etched in a dilute hydrofluoric acid (HF) solution. Such a solution exhibits negligible dark etching. At low powers, the etch rates converge asymptotically, and are almost linear with intensity. In this power region, the etching process is limited by the number of photogenerated carriers reaching the surface. While the etch rates for nitric acid saturate at higher powers, the etch rates for HF remain almost linear; therefore surface removal rates of  $> 500\text{ }\mu\text{m/min}$  can be achieved.

After achieving very fast surface reaction rates, we demonstrated fabrication of structures which could utilize such fast etching. However, dilute HF solution etches quickly and smoothly only within  $3\text{ }\mu\text{m}$  of the surface. As depths exceeded  $3\text{ }\mu\text{m}$ , which corresponds to slower scan rates, the surface becomes nonuniform and etching rates decrease. However, when both HF and

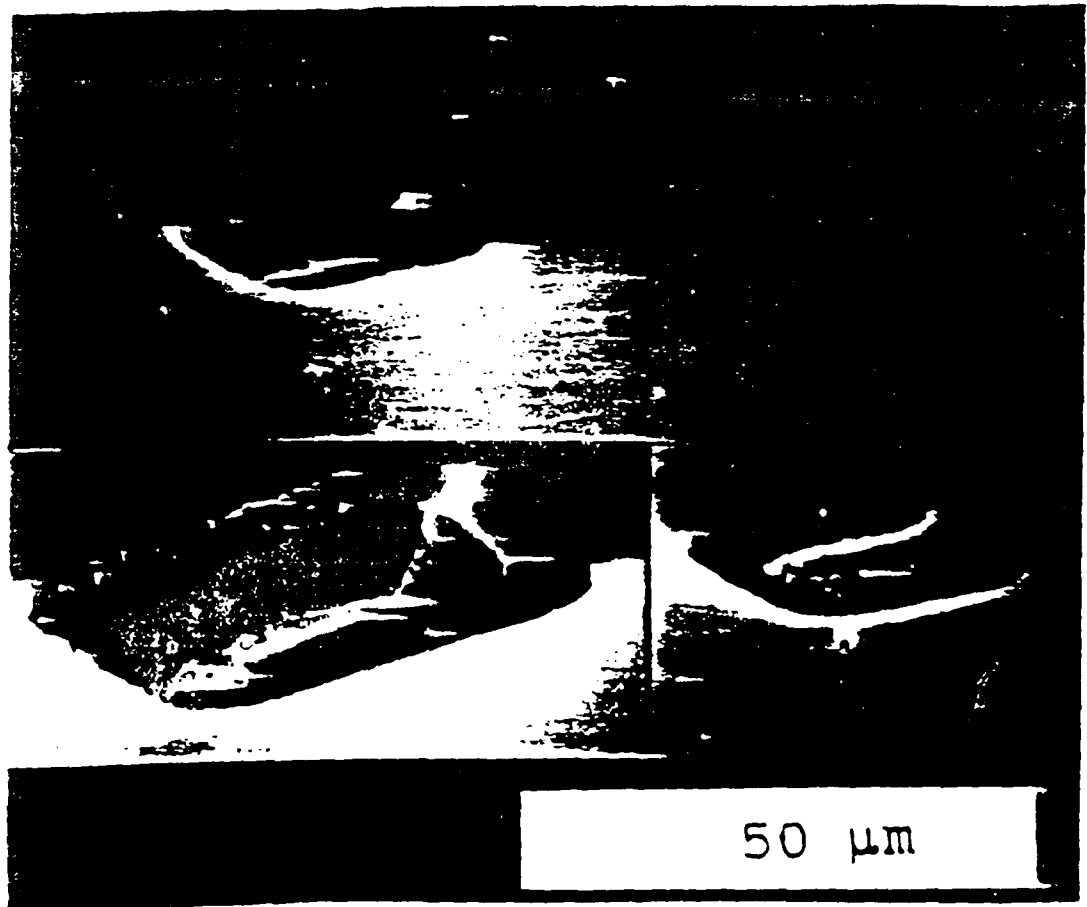


Figure 22. Laser-etched cantilever before and after microcleaving. The inset on the lower left shows an enlargement of the microcleaved facet.

nitric acids are combined, fast etching of deep structures is observed. Whereas the surface etch rates were as fast as with only HF, adding nitric acid did remove products which were left on the surface and allowed deep trenches and structures to be formed. The optimum solution was a mostly HF solution. This small amount of nitric is enough to remove whatever oxide has been left behind by the HF etching.

We were able to demonstrate various applications and uniquely etched structures for this enhanced etch rate of n-GaAs surfaces. High-density wafer-scale etching of a 500- $\mu\text{m}$  square array of 4- $\mu\text{m}$  deep grooves in 10 minutes is depicted in Fig. 23. In addition, 50- $\mu\text{m}$  deep trenches were etched in a 300- $\mu\text{m}$  square array. The entrances are smooth and exhibit waveguide-like etching. Furthermore, we were able to bore via holes through wafers  $\sim 100\text{-}\mu\text{m}$  thick. In order to etch these structures, a 3- $\mu\text{m}$  focused beam was repeatedly rastered quickly back and forth over a square pattern of appropriate size. Such holes would be quite useful for through-wafer metal contacts for microwave devices.

# MICROMACHINING OF GaAs

## LARGE AREA ETCHING

36.

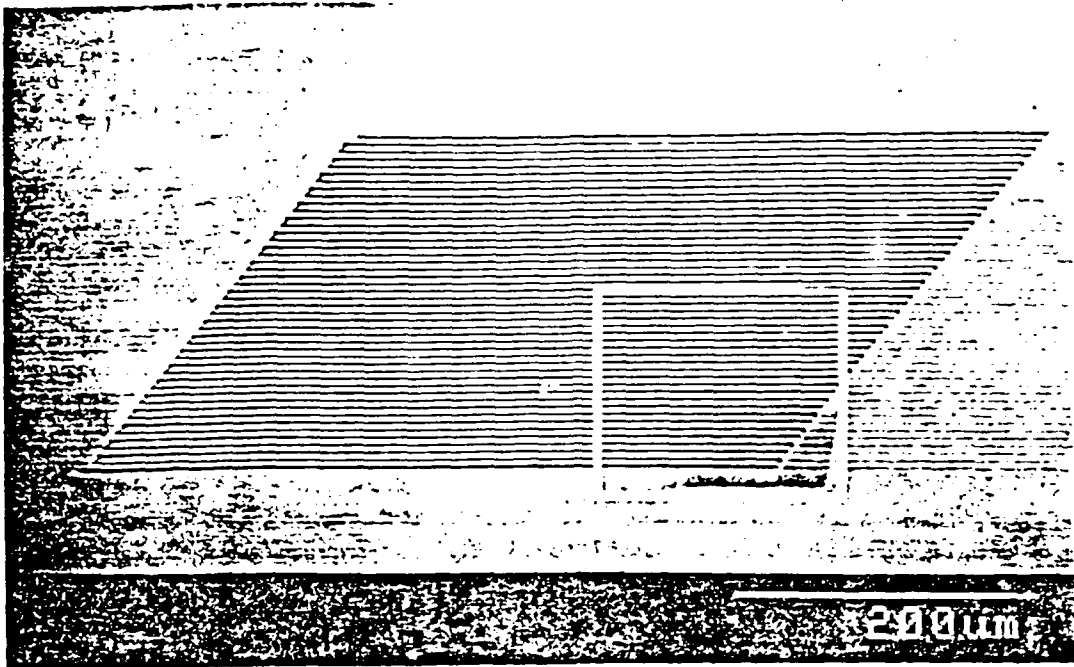


Fig. 23. Large-area GaAs etching of 4-μm deep grooves. The solution was  $\text{HF:HNO}_3:\text{H}_2\text{O} = 2:1:40$ .

C. F. Yu, D. V. Podlesnik, M. T. Schmidt, H. H. Gilgen and R. M. Osgood, "Ultraviolet-Light-Enhanced Oxidation of Gallium Arsenide Surfaces Studied by X-Ray Photoelectron and Auger Electron Spectroscopy," Chemical Physics Letters 130, 301 (1986).

V. Daneu, D. P. DeGloria, A. Sanchez, F. Tong and R. M. Osgood Jr., "Electron-Pumped High Efficiency Semiconductor Laser," Applied Physics Letters 49, 546 (1986).

C. F. Yu, M. T. Schmidt, D. V. Podlesnik and R. M. Osgood Jr., "Optically-Induced, Room-Temperature Oxidation of Gallium Arsenide," Materials Research Society Proceedings, Symposium B, Boston, Massachusetts 75, 251 (1987).

R. M. Osgood Jr., "An Overview of Laser Chemical Processing," MRS Proceedings, Symposium A & B, 74, 75 (1987).

A. E. Willner, O. J. Glembocki, D. V. Podlesnik, E. D. Palik and R. M. Osgood Jr., "Surface Potential Characterization of the Photochemical Etching System by Photorefectance and Electoreflectance Techniques," Proceedings of SPIE, Newport Beach, CA Society of Photo-Optical Instrumentation Engineers, 946, 48 (1988).

T. J. Licata, D. V. Podlesnik, R. Colbeth, R. M. Osgood Jr. and C. C. Chang, "Electrical and Structural Characteristics of Laser Deposited Zn on GaAs," Deposition and Growth: Limits for Microelectronics, Anaheim, CA Gerald Lucovsky in American Vacuum Society Series American Institute of Physics Conference Proceedings No. 167, (1987).

M. T. Schmidt, D. V. Podlesnik, C. F. Yu, R. M. Osgood Jr. and E. S. Yang, "Schottky Contact Characterization of Thin, Excimer-Laser Grown GaAs Oxides," Laser and Particle-Beam Processing, Pittsburgh, PA in Materials Research Society, 101, 421 (1988).

L. Chen, V. Liberman, J. A. O'Neill, Z. Wu and R. M. Osgood Jr., "Ultraviolet Laser-Induced Ion Emission from Silicon," Journal of Vacuum Science Technology A 6, 1426 (1988).

M. T. Schmidt, D. V. Podlesnik, C. F. Yu, X. Wu and R. M. Osgood, "Increased Dependence of Schottky Barrier Height on Metal Work Function Due to a Thin Oxide Layer," Journal of Vacuum Science and Technology B 6, 1436 (1988).

F. Tong, R. M. Osgood, A. Sanchez and V. Daneu, "Electron Beam Pumped Two Dimensional Semiconductor Laser Array with Tilted Mirror Resonator," Applied Physics Letters 52, 1303 (1988).

A. E. Willner, D. V. Podlesnik, H. H. Gilgen and R. M. Osgood, "Photobias Effect in Laser Controlled Etching of InP," Applied Physics Letters 53, 1198 (1988).

R. W. Ade, E. E. Harstead, A. H. Amirfazli, T. Cacouris, E. R. Fossum and P. R. Prucnal et al., "Silicon Photodetector Structure for Direct Coupling of Optical Fibers to Integrated Circuits," IEEE Transactions on Electron Devices 34, 1283 (1987).

R. R. Krchnavek, H. H. Gilgen, P. S. Shaw, T. Licata, J. C. Chen and R. M. Osgood Jr., "Photodeposition Rates of Metal From Metal Alkyls," Journal of Vacuum Science and Technology B 5, 20 (1987).

C. F. Yu, M. T. Schmidt, D. V. Podlesnik and R. M. Osgood, "Wavelength Dependence of Optically Induced Oxidation of GaAs (100)," Journal of Vacuum Science and Technology B 5, 1087 (1987).

A. E. Willner, D. V. Podlesnik and Osgood Jr. R.M., "Inhibition of Laser Induced Photochemical Reactions in Semiconductors by Background Illumination," Conference on Lasers and Electro-Optics, Technical Digest (Optical Society of America), Washington, D.C. 171 (1987).

D. V. Podlesnik, "Characterization of Optically Induced Periodic Structures on Semiconductor Surfaces," Topical Meeting on Lasers in Materials Diagnostics, Technical Digest (Optical Society of America), Washington, DC 95 (1987).

D. V. Podlesnik, "Light-Guided Etching for III-V Semiconductor Device Fabrication," Proceedings of the European Solid State Device Research Conference, Bologna, Italy 462 (1987).

H. H. Gilgen, T. Cacouris, P. S. Shaw, R. R. Krchnavek and R. M. Osgood Jr., "Direct Writing of Metal Conductors with Near-UV Light," Applied Physics B 42, 55 (1987).

M. T. Schmidt, D. V. Podlesnik, H. L. Evans, C. F. Yu, E. S. Yang and J. R. M. Osgood, "The Effect of UV-Grown Oxide on Metal-GaAs Contacts," American Vacuum Society Meeting, Anaheim, CA Journal of Vacuum Science and Technology A, (1987).

C. F. Yu, M. T. Schmidt, D. V. Podlesnik, E. S. Yang and R. M. Osgood Jr., "Ultraviolet-Light-Enhanced Reaction of Oxygen with Gallium Arsenide Surfaces," AVS Symposium Proceedings, Journal of Vacuum Science and Technology A, 6, 754 (1988).

D. V. Podlesnik, and H. H. Gilgen, "Laser-Controlled Aqueous Etching of Semiconductors (book chapter)," in Photochemical Materials Processing, K. Ibbs and R.M. Osgood, (Cambridge University Press, Cambridge, 1988).

M. N. Ruberto, A. E. Willner, D. V. Podlesnik and R. M. Osgood Jr., "Photogenerated Carrier Confinement During the Laser-Controlled Aqueous Etching of GaAs/AlGaAs Multilayers," Materials Research Society, (1988).

A. E. Willner, D. J. Blumenthal, M. N. Ruberto, D. V. Podlesnik and R. M. Osgood Jr., "Laser Fabricated GaAs Waveguiding Structures," Applied Physics Letters 54, 19 (1989).

A. E. Willner, M. N. Ruberto, D. V. Podlesnik and R. M. Osgood Jr., "Laser Direct Writing of Integrated Optical Components in the GaAs/AlGaAs System," Meeting of the Electrochemical Society, (1988).

G. V. Treyz, R. Scarmozzino and R. M. Osgood Jr., "Deep Ultraviolet Laser Etching of Vias in Polyimide Films," Applied Physics Letters 55, 346 (1989).

M. T. Schmidt, Q. Y. Ma, D. V. Podlesnik and R. M. Osgood Jr., "Chemically Modified GaAs Schottky Barrier Variation," Journal of Vacuum Science and Technology B 7, 980 (1989).

M. N. Ruberto, A. E. Willner, D. V. Podlesnik and R. M. Osgood Jr., "Effect of Carrier Confinement on the Laser-Enhanced Etching of GaAs/AlGaAs Heterostructures," Applied Physics Letters 55, 984 (1989).

B. Quiniou, R. Scarmozzino, Z. Wu and R. M. Osgood Jr., "Photoemissive Scanning Microscopy of Doped Regions on Semiconductor Surfaces," Applied Physics Letters 55, 481 (1989).